# Recent Advances in the Preparation and Application of DNA-Encoded Metal Nanoclusters

**Fang Yin** [1,2] ⓘ, **Jiangtao Ren** [2,]* ⓘ **and Erkang Wang** [1,2,]*

1 College of Chemistry, Jilin University, Changchun 130012, China
2 State Key Laboratory of Electroanalytical Chemistry, Changchun Institute of Applied Chemistry, Chinese Academy of Sciences, Changchun 130022, China
* Correspondence: jiangtaoren@ciac.ac.cn (J.R.); ekwang@ciac.ac.cn (E.W.); Tel.: +86-431-85262003 (E.W.)

**Abstract:** DNA as an intriguing organic ligand has been widely employed for synthesizing metal nanoclusters and engineering their properties. This review aims to present recent progress on DNA-encoded metal (Ag, Cu, Au, Ag/Pt, Cu/Ag, etc.) nanoclusters (DNA-MNCs), focusing on their applications in the fields of analysis, logic operation, and therapy based on properties including fluorescence, electrochemiluminescence (ECL), and antibacterial and catalytic activity, and summarizes the attractive features of the latest research. The key points are briefly described as follows. (1) Analytical systems have been constructed based on fluorescence regulation, and nuclease-assisted and enzyme-free amplification strategies have been extensively adopted with fluorescent DNA-MNCs for amplified analysis. (2) DNA-MNCs may play more than one role (emitter, quencher, or catalyst) in ECL-based analytical systems. (3) Apart from antibacterial activity, DNA-MNCs also possess apparent catalytic capability, such as enzyme-like activity (i.e., nanozymes), which has been applied in colorimetric systems. (4) Reversibly regulating the catalytic activity of DNA-MNCs has been attained with DNA systems. It is believed that through in-depth investigation of the relationship between atomic structure and property, more novel DNA-MNCs will be explored and applied in the future.

**Keywords:** DNA; metal nanoclusters; fluorescence; catalytic activity; bioanalysis; antibacterial

## 1. Introduction

Deoxynucleic acid (DNA), as the main carrier and transmitter of genetic information in living systems, consists of four different deoxynucleotide monomers containing phosphate groups, deoxyribose rings, and nitrogen-containing bases, thymine (T), adenine (A), guanine (G), and cytosine (C). A single-stranded DNA (ssDNA) is generated by phosphodiester bonds between monomers. Apart from the common double helix DNA structure, DNA strands can form different secondary structures under certain conditions, such as hairpin, i-motif, triplex, and G-quadruplex, via classical Watson-Crick base pairing and unique Hoogsteen hydrogen bonds. Attributing to its diversity and programmability, DNA has been utilized as a capping ligand for synthesizing nanomaterials and engineering their properties, resulting in DNA-encoded nanomaterials [1]. Metal (Ag, Au, Cu, etc.) nanoclusters (MNCs) with sub-nanometer sizes have been prepared with DNA strands as templates and widely studied in the past decade due to prominent optical, catalytic, or antibacterial features [2–5]. The physicochemical characteristics of MNCs are closely related to DNA templates and can be adjusted with dictated DNA strands, and thus so-called DNA-encoded MNCs (DNA-MNCs) can be defined and have been developed. So far, much progress has been made with the study of DNA-MNCs in the areas of, for example, DNA-based biosensing and logical computing systems [6]. Many reviews have been reported on DNA-MNCs, such as on DNA-templated silver nanoclusters (DNA-Ag NCs) [7–9] and copper nanoclusters (DNA-Cu NCs) [10], and related synthetic methods and applications

were summed up. In most of these reviews, a specific type of MNCs is focused on, and respective fluorescent properties and analytical applications are described in detail.

Herein, we will focus on recent research progress on DNA-MNCs, including DNA-Ag NCs, DNA-Cu NCs, DNA-templated gold nanoclusters (DNA-Au NCs), DNA-templated silver/platinum nanoclusters (DNA-Ag/Pt NCs), etc., summarize their common and intriguing features from diverse properties (e.g., fluorescence and catalysis) to unique applications, and inspire researchers to explore more complicated and intelligent DNA-MNC-based systems and expand the applicable scope of MNCs.

## 2. Synthetic Methods of MNCs

In the last two decades, dramatic advances have been achieved in developing new synthetic methods for MNCs, including top-down and bottom-up methods [11–14]. Ligand-mediated etching of metal nanoparticles (MNPs) is one of the widely used top-down approaches for synthesizing MNCs [12,13]. The excess ligands, such as glutathione [13]), diphosphine [15], and BSA [14], have been utilized in the etching process to obtain ultra-small MNCs. As for the bottom-up approach, which is the atom-to-clusters synthetic method, metal ions are reduced to metal atoms by virtue of reducing reagents [16–19], illumination [20–23], electrochemistry [24–26], sonication [27,28], microwave [29,30], etc., and capping ligands are usually required to reduce huge surface energy and stabilize NCs [31,32]. Brust and co-workers [16] first reported the synthesis of gold nanoclusters (Au NCs) with $BH_4^-$ as a reducing agent and $C_{12}H_{25}SH$ as a protecting ligand. Suresh Kumar Kailasa et al. synthesized blue fluorescent Au NCs with two ligands, 6-thioguanine and tryptophan [33]. Many factors can affect the size and surface properties of MNCs, such as the ligand to metal molar ratio, types of reducing agents and stabilizing ligands, time and temperature of reaction, etc. The nature of protecting ligands is quite vital for synthesis of MNCs. Organic scaffolds, especially biomolecules, such as thiolates [34], polymers [35–39], proteins [40–45], and DNA [38,39], are widely used as protecting ligands in the chemical reduction processes [46–48]. Small-molecule thiolates, as one of the most commonly used protective agents, are capable of effectively controlling the size and shape of MNCs. Polymer scaffolds ensure a high degree of structural stability, and protein as a ligand can provide rich functionality and adjustability for MNCs. Since the silver nanowire with DNA as a template was produced, DNA has been regarded as one of the most excellent scaffolds to mediate the synthesis of MNCs [49]. Nucleobases and the negatively charged backbones of DNA provide various binding sites for metal ions through electrostatic or coordination interactions. It has been verified that these nitrogen groups from nucleobases could coordinate with many metal ions. $Ag^+$-binding sites are the N3 in pyrimidines and N7 in purines [50,51], $Cu^{2+}$ has a high affinity to the N3 in the T base [52], and $Au^{3+}$ could be stabilized at the N7 site of the A base [53,54]. Based on these interactions between DNA and metal ions, metal ions could be reduced to metal atoms, which then accumulate into stable NCs. Moreover, in contrast to other scaffolds, due to its prominent structural diversity and programmability, DNA not only has acted as a template for synthesis of MNCs, but also can be harnessed for precisely adjusting (i.e., encoding) structures and properties of MNCs and acquiring diverse DNA-MNCs.

Dickson et al. first used ssDNA as a template and synthesized DNA-Ag NCs [17]. Our group, for the first time, prepared DNA-Ag NCs with double-stranded DNA (dsDNA) templates and demonstrated the highly sequence-dependent feature and capability of single nucleotide mutation identification [55]. Moreover, our group theoretically and experimentally validated that among four DNA monomers, only deoxycytidine (dC)-protected Ag NCs emitted strong fluorescence [35]. Thus, C-rich DNA templates are commonly utilized for synthesis of fluorescent Ag NCs [56]. Thereafter, various DNA sequences have been applied to synthesize DNA-Ag NCs with various fluorescent properties. It is worth noting that fluorescence stability of DNA-Ag NCs is associated with binding affinity between $Ag^+$ and DNA templates. In contrast to DNA templates with secondary DNA structures, including G-quadruplex, duplex, and i-motif, coiled DNA-capped DNA-Ag

NCs revealed the most stable fluorescence, namely, G-quadruplex < duplex < i-motif < coiled C-rich strand [36,57]. Besides DNA-Ag NCs, other DNA-MNCs have been prepared with DNA strands. Fluorescent DNA-Au NCs were obtained with ssDNA as a template and dimethylamine borane (DMAB) as a reducing agent [19]. Fluorescent DNA-Cu NCs could be synthesized with dsDNA [38] and poly T ssDNA [39], owing to weak interactions between $Cu^{2+}$ and T bases.

## 3. Applications of DNA-MNCs Based on Their Diverse Properties

### 3.1. Fluorescence

Owing to their unique electronic structure and surface plasmon resonance effect, MNCs, mainly including Ag NCs, Cu NCs, and Au NCs, emit obvious fluorescence [58–60]. DNA, as a powerful molecular tool, has been utilized for preparing fluorescent DNA-MNCs and encoding their fluorescence properties. Consequently, multifarious DNA-MNCs have been explored and applied for construction of biosensors and logic gates (Table 1).

**Table 1.** Spectral characteristics of representative fluorescent DNA-MNCs in recent years and their applications in recent years.

| Template [1] | Type of DNA-MNCs | Excitation/Emission Maxima (nm) | Particle Size (nm) | Application | Refs. |
|---|---|---|---|---|---|
| 5′-ACA GAC ATC TCT TCT ATA GTG TAG **TTT TGC CTT TTG GGG ACG GAT A**-3′ | DNA-Ag NCs | 500/560 and 570/620 | 3.3 | Detection of $Hg^{2+}$ | [61] |
| 5′-**CCT CCT TCC TCC** TTT GTA TTG CGC CGC TCT TTC GGA ATG CCG GCG CTT AT**C CCT TAA TCC CC**-3′ | DNA-Ag NCs | 495/549 and 580/641 | <10 | Detection of two ARGs (tet-A and sul-1) | [62] |
| 5′-**CCC TTA ATC CCC** TGA GGT AGT AGG TTG TAT AGT T-3′ | DNA-Ag NCs | 560/625 | <10 | Detection of let-7 miRNAs | [63] |
| 5′-**CAC CGC TTT**-3′ | DNA-Ag NCs | 570/670 | 2.3 | Detection of *invA* gene (*S. typhi*) | [64]. |
| 5′-**AAT TTT AAA TAA TAT CCC CTA ATT CCC**-3′ | DNA-Ag NCs | 530/635 | 5 | Detection of bacterial DNA | [65] |
| 5′-**CCC CCC CCT TAA TCC CCC CC**-3′ | DNA-Ag NCs | 560/610 | 1.8–2.6 | Detection of circRNA | [66] |
| 5′-**CCC TTA ATC CCC** AAT TGT CCG ACC TGC AGT GAT GAC AAA **ACC CCC TAA TTC CCC C**-3′ | DNA-Ag NCs | 565/630 | 3.2 | Logic operation (XORˆXNOR, etc.) | [67] |
| 5′-**CCC TTA ATC CCC GTG** CTT CCT TAT TGA TTT GTG TAT CAA TAA GGA AGA AGC CCT TCA GCG GCC AGT AGC A**GG GTG GGG TGG GGT GGG G**-3′ 5′-**CCT CCT TCC TCC** TTG AAC TCT GCT TAA ATC CAG CTA ATT CTG GAT TTA AGC AGA GTT CAA AAG CCC TTC AGC **CCC TAA CTA CCC**-3′ | DNA-Ag NCs | 495/518 and 595/664 | - | Detection of Fusion Gene Isoforms | [2] |
| 5′-**CCC TTA ATC CCC** ATA CAC GCA CCT CAC CAC GAC CAC TCG CGA ATC TGT CCT GGA CTG-3′ | DNA-Ag NCs | - | 4 | Determination of Acrylamide (AAm) | [68] |

**Table 1.** *Cont.*

| Template [1] | Type of DNA-MNCs | Excitation/Emission Maxima (nm) | Particle Size (nm) | Application | Refs. |
|---|---|---|---|---|---|
| dsDNA:5′-**TAC TCA TAC GCT CAT ACG TTC ATC ACG ACT AC**A GTT GAG AAT ACG AGT-3′ | DNA-Cu NCs | 351/594 | 6.25 | Detection of biothiol and $S^{2-}$ | [69] |
| 5′-**TTT TTT TTT TTT TTT TTT TTT TTT TTT TTT**-3′ | DNA-Cu NCs | 340/630 | <5 | Logic operation (IMPLICATION etc.) and detection of K+ and microRNA 122b | [70] |
| 5′-ATG GTG GGG **TTT TTT TTT TTT TTT TTT TTT** ACC CCA CCA TTG TCA CAC TCC A-3′ | DNA-Cu NCs | 340/671 | >5 | Detection of miRNA-122 | [71] |
| 5′-**TTT TTT TTT TTT TTT TTT TTT TTT TTT TTT** GT/i8oxodG/CGA TCA GTG CTG A-3′ | DNA-Cu NCs | 340/625 | 4 | Detection of Formami- dopyrimidine DNA Glycosylase (Fpg) | [72] |
| 40T: **TTT TTT TTT TTT TTT TTT TTT TTT TTT TTT TTT TTT TTT T** | DNA-Cu NCs | 340/585 | <5 | Detection of survival motor neuron (SMN) gene | [73] |
| 30T: **TTT TTT TTT TTT TTT TTT TTT TTT TTT TTT** | DNA-Cu NCs | 340/650 | 2.3–2.7 | Detection of Hepatitis B Virus (HBV) | [74] |
| 5′-**AAA AAA AAA AAA AAA AAA AAA AAA AAA** AAA-3′ | DNA-Au NCs | 280/475 | $3.67 \pm 1.39$ | Detection of trypsin | [75] |

[1] The sequences in bold are the nucleation sites of MNCs.

### 3.1.1. Regulating Fluorescence of DNA-MNCs for Logic Operation and Analysis

As mentioned above, fluorescent properties of DNA-MNCs depend on sequences of DNA templates [17,76]. Diverse DNA-Ag NCs, which emitted blue, green, yellow, or red fluorescence, were prepared with different C-rich sequences [17]. Moreover, post-regulating fluorescence of DNA-Ag NCs has been attained via stimulus-responsive DNA allostery. Our group designed one stimuli-responsive DNA-Ag NC with a poly C-containing hairpin DNA template (HP26), which was capable of transforming into a new structure with G-quadruplex and/or i-motif upon addition of $K^+$ or $H^+$ and regulated fluorescence of HP26-templated Ag NCs in multiple logic manners, leading to elementary logic gates [77]. Similarly, fluorescent logic devices were also constructed by dual-responsive Poly T-Cu NCs [70].

It is worth noting that nonfluorescent DNA-Ag NCs can be lit up by adjacent G-rich DNA strands [61,63] or ligand displacement [37]. In addition, spectral conversion of DNA-Ag NCs by adjacent poly G sequence occurred, namely from yellow-emitting silver nanoclusters (Y-Ag NCs) to red-emitting silver nanoclusters (R-Ag NCs), no matter what the hybridization sequence was [61] (Figure 1A). The mechanism of the spectral conversion was validated as the formation of new Ag NCs and the interaction between the two Ag NCs. Based on this universal phenomenon, a ratiometric nanoprobe was developed for detection of $Hg^{2+}$. In the presence of $Hg^{2+}$, two DNA strands can hybridize with each other via thymine-Hg-thymine base pairs, and the Y-Ag NCs were transformed into R-Ag NCs due to the proximity of the poly G sequence. Thus, a significant spectral redshift was observed for quantitation of target $Hg^{2+}$. In contrast to many ratiometric probes, the method can be applied to actual water samples with good sensitivity and selectivity, many simple preparation steps are required, and a low detectable minimum target concentration of 0.01 μM was obtained. Benefiting from their multifarious fluorescence properties, DNA-Ag NCs have been employed for multiple analyses. A novel fluorescence sensing strategy was developed for detection of two ARGs (tet-A and sul-1) based on fluorescence variation

of two types of DNA-Ag NCs by the G-rich sequence in proximity (Figure 1B) [62]. The chameleon DNA-Ag NCs (H1-Ag NCs) carried two Ag NCs at 5′ and 3′ ends and can be hybridized with H2 and bridging DNA, yielding a three-way junction, which can assemble to a linear structure in the presence of tet-A or sul-1. Due to the proximity of a G-rich sequence of H2 to Ag NCs, fluorescent enhancement at 549 nm or 641 nm was observed and utilized for separate detection of tet-A and sul-1. Simultaneous analysis of the two ARGs can be attained by simply monitoring fluorescence emission at 549 nm and 641 nm. This strategy exhibited good applicability in detecting actual samples containing complex components and holds potential for rapid quantitative detection of ARGs in various environmental media.
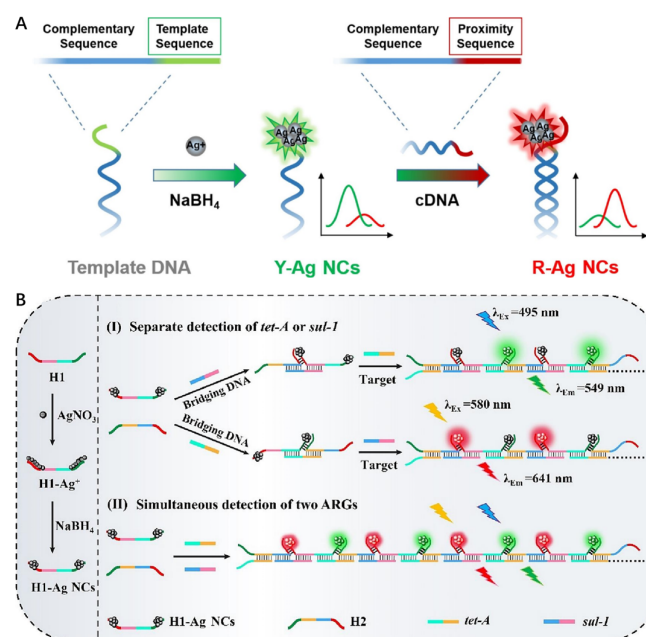


**Figure 1.** (**A**) Schematic illustration of a universal ratiometric nanoprobe based on spectral conversion of DNA-Ag NCs due to adjacent poly G sequence after hybridization, reproduced with permission from Ref. [61]. Copyright 2022, Elsevier B.V. Publishers. (**B**) A scheme illustrating detection of two ARGs in aquatic environments based on chameleon DNA-Ag NCs, due to adjacent poly G, reproduced with permission from Ref. [62]. Copyright 2023, Elsevier B.V. Publishers.

Moreover, varieties of bioanalytical platforms have been constructed [2,64,78] on the basis of direct fluorescence regulation of DNA-MNCs. For example, our group adopted strand exchange reaction to reversibly regulate fluorescence of dsDNA-Ag NCs [79] and developed a DNA-Ag NC-based molecular beacon for detection of virus genes [80]. Dadmehr et al. inserted six C bases in a DNA strand, which was capable of recognizing a target DNA sequence from the CpG islands of adenomatous polyposis coli tumor suppressor gene promoter [81]. The resulting dsDNA was utilized as a template to prepare DNA-Ag NCs with strong fluorescence, but the fluorescence turned weak when the target DNA was methylated, so unmethylated and methylated DNA strands could be distinguished. It is well-known that conformation changes of DNA templates can cause alteration of fluorescence emission. Based on the strong electrostatic interaction between ssDNA-Au NCs and cationic polyelectrolytes, a fluorescence method for trypsin determination was developed [75]. Due to the electrostatic interaction between protamine and ssDNA templates, the conformation of ssDNA changed, resulting in enhanced fluorescence emission. Upon addition of trypsin, fluorescence decreases from ssDNA-Au NCs were observed due to the breakdown of protamine by trypsin. They also extended this method to determine trypsin in human serum samples, with recoveries between 98.7% and 103.5% and relative standard deviation (RSD) between 3.5% and 4.8%.

3.1.2. Enzyme-Assisted Amplification in Biosensing Systems with DNA-MNCs as Reporters

In recent years, various amplification strategies, such as polymerase chain reaction (PCR) [82], loop-mediated isothermal amplification (LAMP) [83], and nuclease-assisted signal amplification (DSNSA) [63], have been successfully integrated into DNA-Ag NC-based analytical systems to achieve a limit of detection (LOD) as low as fM or aM. For example, a very simple and sensitive homogeneous detection strategy for microRNA (miRNA) has been established based on the fluorescence enhancement of Ag NCs by G-rich DNA and in combination with DSNSA [63]. As shown in Figure 2A, a DNA probe, DNA-Ag NCs, and a duplex-specific nuclease (DSN) were involved. The presence of target miRNA (let-7a) can trigger a DSNSA reaction, leading to degradation of captured DNA probes and weakening of the fluorescence enhancement of DNA-Ag NCs by adjacent poly G sequence (purple line). The proposed method achieved excellent sensitivity (LOD: 80 aM) and a dynamic detection range exceeding four orders of magnitude. The CRISPR-Cas12a protein, as a powerful diagnostic tool, has been introduced into nucleic acid-based biosensing systems. As shown in Figure 2B, a novel sensitive fluorescent biosensor was developed for HBV detection, using CRISPR-Cas12a enzyme and DNA-MNCs (Au NCs, Ag NCs and Cu NCs) as luminescent nanoprobes [74]. In the presence of HBV targets, Cas12a's trans cleavage ability can be activated to degrade DNA probes, thereby inhibiting the formation of DNA-MNCs and leading to fluorescence decrease. This analytical method was used to detect HBV DNA targets in human serum. Additionally, a multifunctional biosensing platform called SCENT Cas (DNA-Ag NCs authorized nucleic acid testing using CRISPR/Cas12a) was developed for ultra-sensitive and rapid detection of pathogenic bacteria [64].
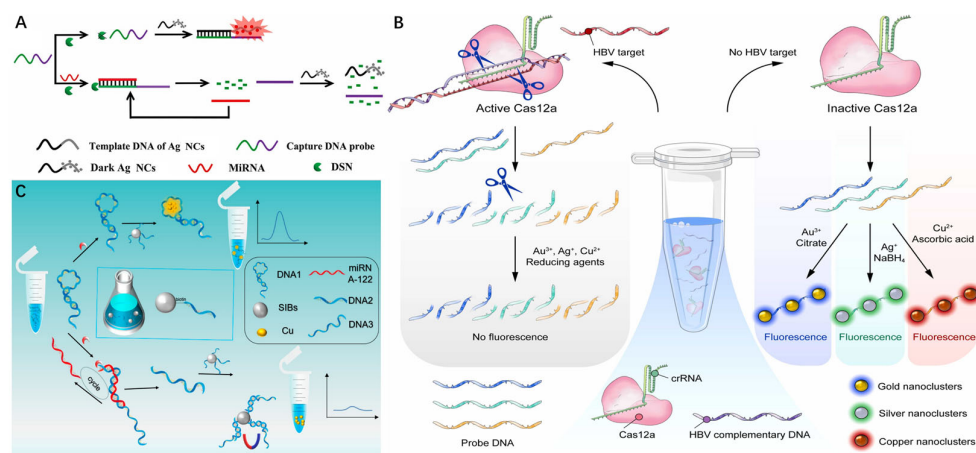


**Figure 2.** (**A**) The principle of a simple and sensitive miRNA detection strategy based on inhibition of DSNSA on the fluorescence enhancement, reproduced with permission from Ref. [63]. Copyright 2022, Elsevier B.V. Publishers. (**B**) A sensing system for HBV DNA detection by virtue of CRISPR-Cas12a enzyme and DNA-MNCs luminescent nanoprobes, reproduced with permission from Ref. [74]. Copyright 2022, Elsevier B.V. Publishers. (**C**) DNA-Cu NC-based and Exo III-assisted amplified detection of miRNA-122, reproduced with permission from Ref. [71]. Copyright 2023, MDPI Publishers.

Exonuclease III (Exo III) has often been adopted with DNA-Ag NCs to construct amplified sensing systems. Fluorescent DNA-Cu NCs were prepared with a poly T-containing hairpin DNA (DNA1) as a template [71] (Figure 2C). In the presence of the miRNA-122 target, DNA1 was opened due to loop hybridization and was then digested from the 3′end by Exo III. At the same time, the released miRNA-122 underwent the next cyclic amplification reaction, finally yielding a number of residual DNA (DNA3), which could be separated by DNA2-modified magnetic beads (SIB) via hybridization between DNA2 and

DNA3. As a result, decreased fluorescence from DNA-Ag NCs was observed and applied for miRNA-122 determination, and its detection limit was 0.46 nM.

Multiple enzymes are often utilized to design DNA-based amplified circuits. The activity of Fpg was determined by combining phosphate group (P) regulated multi-enzyme catalysis with fluorescent DNA-Cu NCs [72]. The Fpg biosensor consisted of ssDNDA-1 and ssDNA-2 and two exonucleases, Lambda Exonuclease (λ Exo) and Exonuclease I (Exo I). In the absence of Fpg, a DNA hybrid of the two ssDNAs was decomposed by λ Exo and Exo I, and no fluorescent DNA-Cu NCs were produced. Upon addition of Fpg, 3 'P of poly (T) ssDNA impeded its degradation by Exo I, leading to formation of DNA-Cu NCs and high emission. The method was utilized for detecting Fpg in serum samples and cell lysates and exhibited its great application potential in practical and clinical analysis.

Moreover, multiple-fold amplification strategies have been designed in biosensing systems with DNA-MNCs as reporters. As shown in Figure 3A [64], the species-specific invA gene of Salmonella typhimurium (S. typhi) was amplified using isothermal LAMP, and the products activated CRISPR/Cas12a to cleave converter ssDNA, which can influence the dual fluorescence emission of DNA-Ag NCs through hybridization. In the absence of the invA gene, strong red fluorescence and minimal green fluorescence were observed. Upon addition of the invA gene, converter ssDNA was cleaved, resulting in a decrease of red fluorescence and an increase of green fluorescence. Therefore, pathogenic bacteria can be determined according to the signal ratio of red and green fluorescence. Spinal muscular atrophy (SMA) is a serious genetic disease that causes infant death in clinical practice, and testing of the SMN gene is an effective approach to SMA diagnosis. A simple SMN fluorescence detection method was established based on luminescent poly T-Cu NCs and cascaded PCR and RCA amplification techniques (Figure 3B) [73]. Numerous Poly T sequences were produced after PCR and RCA reactions and utilized as templates to form fluorescent DNA-Cu NCs with introduction of $CuSO_4$ and sodium ascorbate. Fluorescence of Cu NCs was only detected in samples containing the SMN1 gene. After optimizing the experimental conditions, this highly effective method was successfully applied for identifying clinical DNA samples, including four SMA patients, four carriers, and 57 random individuals.

### 3.1.3. Enzyme-Free Amplification in DNA-MNC-Based Biosensing Systems

In addition to the above enzyme-assisted amplification strategies, enzyme-free and low-cost DNA amplification circuits, such as catalytic hairpin assembly (CHA) [84] and hybridization chain reaction (HCR) [85], have been introduced to DNA-MNC-based biosensing platforms. In CHA reactions, the target as a catalyst can circularly trigger DNA assembling of DNA fuels cascade, thereby generating significant signal amplification. By coupling CHA with DNA-Ag NCs, a simple, enzyme-free, and label-free method was constructed for detecting an universal sequence of sulfate-reducing bacteria (SRB-385), which is one of the most common marine corrosive microorganisms (Figure 4A) [65]. The sequence II–V and II'–V' are complementary sequences that can be specifically identified to form the T + P1 + P2 + P3 structure, and the target substance can participate in the reaction cycle while promoting CHA reactions. The bacterial DNA target triggered a CHA reaction among P1, P2, and P3, and three-way DNA junctions with free C-rich ends were yielded, which can act as templates for synthesizing DNA-Ag NCs, leading to high fluorescence because of G-rich DNA hybridization. Consequently, as the concentration of target DNA increased, the fluorescence of DNA-Ag NCs gradually increased. As low as 19.95 fM target can be detected, and the sensitivity of this method has increased by approximately three orders of magnitude in contrast to the analytical system without CHA. The sensitive and selective detection of circRNA can greatly promote the early diagnosis of human diseases. An isothermal amplification system was proposed based on dual CHA and chameleon DNA-Ag NCs for label-free ratiometric detection of circRNA (Figure 4B) [66]. Two CHA cycles (CHA1 and CHA2) were involved; CHA1 can be specifically triggered by the target $T_{DNA}$ to form a dsDNA (H1/H2) product, and the released $T_{DNA}$ can trigger a new

round of CHA1 cycle. The H1/H2 double-stranded product caused red fluorescence of hairpin DNA-Ag NCs to darken due to breakage of the hairpin structure and served as an initiator to further activate downstream CHA2 to produce another dsDNA complex (H3/H4), which induced other dark DNA-Ag NCs to approach a G-rich sequence, leading to an increase of green fluorescence, in short, turning black fluorescence H3-Ag NCs into bright green fluorescence H3/H4-AgNCs. Thus, circRNA was sensitively detected and visually distinguished by measuring the significant changes in the ratio of green to red fluorescence intensity. In addition, this new method can be used as a universal strategy for analyzing different types of circRNAs, demonstrating its enormous potential for detecting low abundance biomarkers in various clinical studies.
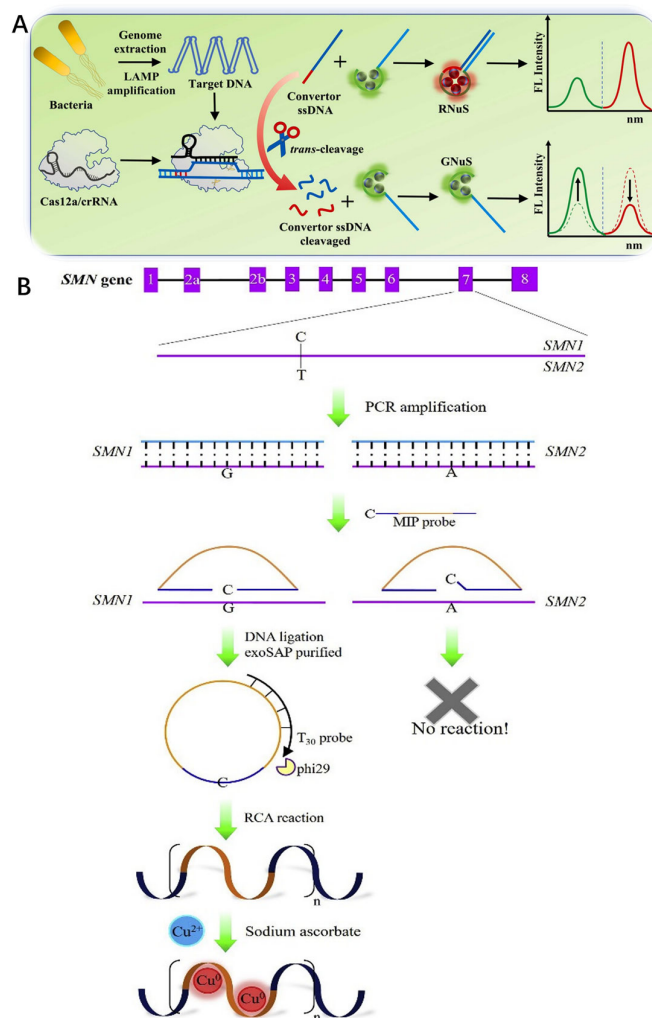


**Figure 3.** (**A**) The principle of a multifunctional biosensing platform for bacterial gene detection, in combination with LAMP, CRISPR/Cas12a, and DNA-Ag NCs, reproduced with permission from Ref. [64]. Copyright 2022, Elsevier B.V. Publishers. (**B**) The principle of SMN detection for diagnosis of SMA by using PCR, RCA, and fluorescent poly T-Cu NCs, reproduced with permission from Ref. [73]. Copyright 2020, Elsevier B.V. Publishers.
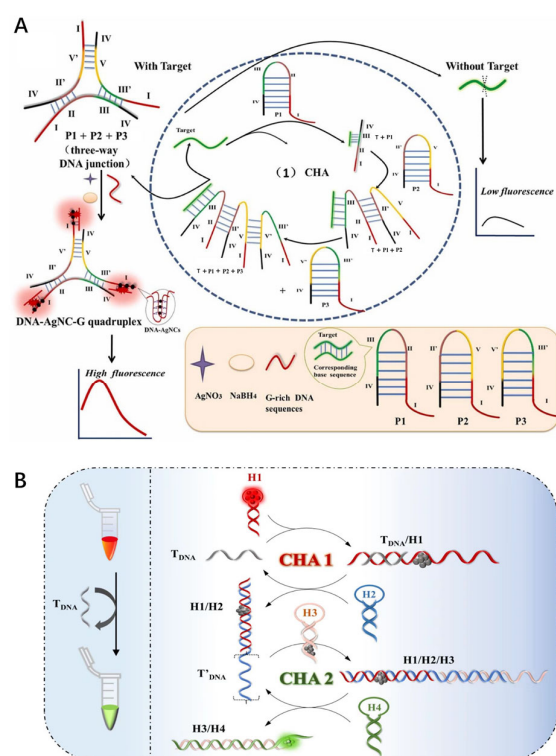
**Figure 4.** (**A**) The principle of a label-free and enzyme-free method for DNA detection based on CHA and DNA-Ag NCs, reproduced with permission from Ref. [65]. Copyright 2022, Elsevier B.V. Publishers. (**B**) The cascaded CHA for ratiometric detection of circRNA with chameleon DNA-Ag NCs, reproduced with permission from Ref. [66]. Copyright 2022, Elsevier B.V. Publishers.

### 3.1.4. DNA-MNC-Based Dimeric Structures and Their Amplifications

Varieties of bioanalytical platforms have been fabricated, and meanwhile, the relationship between structure and photophysical property has been explored. In early 2018, the first crystal structure DNA-Ag NC was reported [86]. One $Ag_8$ cluster with green emission was described in this work, and it was confined by two DNA strands. The X-ray crystal structure of $Ag_{16}$ emitting NIR was also observed in another study, and it was located between two 10-mer DNA strands [86,87]. Similarly, a dimeric structure was verified for one fluorescence DNA-Ag NCs ($Ag_{12}$) in which two DNA hairpins were bridged by an $Ag_{12}$ cluster in a head-to-head mode [88]. The secondary structure of DNA is crucial for DNA-Ag NCs, which in turn can stabilize secondary DNA structures, such as hairpin DNA, dsDNA, and parallel motif DNA triplets. Recently, Ag NCs between two C-rich rings can be used as nanorivets, which were reported for designing non-standard DNA origami beyond Watson-Crick base pairing [89]. DNA triplex-encapsulated Ag NCs can undergo photophysical conversion, and the fluorescence was switched on in a non-alkaline environment because of the dimerization of triplet DNA riveted by Ag NCs. In addition, it has also been found that Ag NCs riveted triplet DNA and hairpin DNA form heterodimers, emitting orange fluorescence. These works provide novel structural tips for researchers to study and explore different fluorescence logic and sensing systems.

Our group acquired one type of DNA-Ag NC-based dimeric structure (H-Ag NCs) with a DNA template of hairpin DNA containing two C-rich emitter-nucleation sequences (Figure 5A) [67], and two fluorescence emissions at 565 nm and 630 nm were produced. Moreover, the fluorescence can be regulated via loop hybridization with an input of IN1, leading to inverse intensity changes at the two wavelengths. Based on the alteration of dimeric DNA-Ag NCs and consequent fluorescence change, a series of concomitant contrary logic gates, e.g., INHIBIT^IMPLICATION, XOR^XNOR, and MAJORITY^MINORITY, and complicated logic circuits (e.g., parity generators and checkers) were obtained. This work provided one new approach to fabricating cost-effective logic systems. On the basis of

head-to-head dimerization of DNA-Ag NCs and concomitant fluorescence change, an in situ imaging platform was developed for rapid identification of fusion gene subtypes and subtype (e13a2 and e14a2) [2]. As shown in Figure 5B, four DNA-Ag NC-loaded hairpin DNA fuels (ADHA1, ADHA2, ADHA3, and ADHA4) were prepared for recognizing e13a2 and e14a2 with CHA1 and CHA2, respectively. As a result, duplex products with two DNA-Ag NC emitters were obtained with green emission and utilized for e13a2 quantitation; moreover, the duplexes with two groups of dimeric DNA-Ag NCs as deep red emitters were employed for e14a2 detection and can be transformed into those with strong orange emission in the presence of $Ag^+$. Accordingly, fluorescence imaging of e13a2 (green), e14a2 (orange), and e13a2/e14a2 (orange/green) were realized.
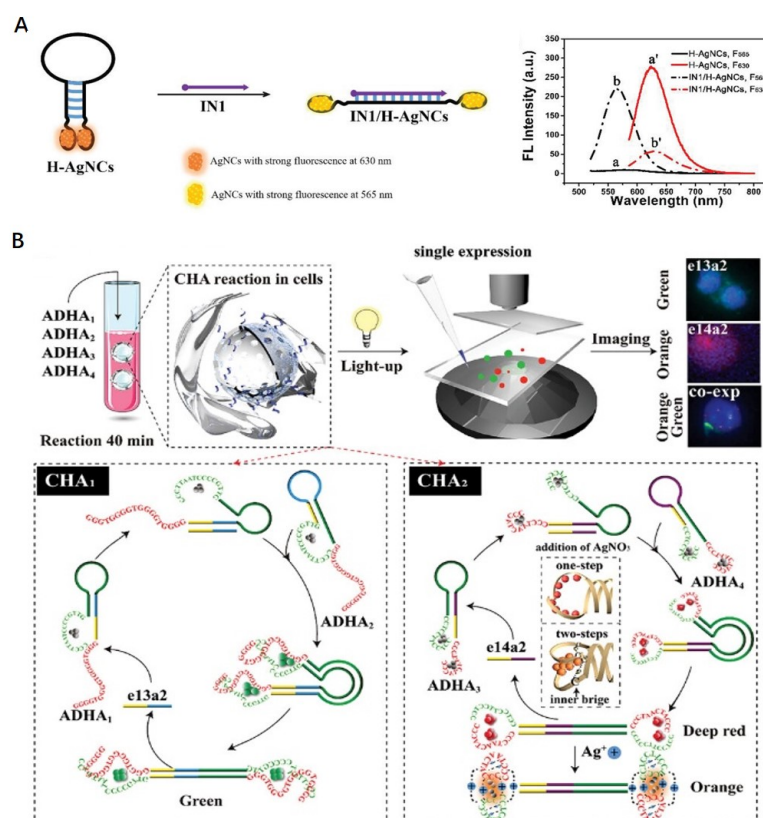


**Figure 5.** (**A**) A scheme illustrating a logic device based on dimeric DNA-Ag NCs using a hairpin DNA template with two emitter-nucleation sequences, unique fluorescence property, and input-stimulated emission change, reproduced with permission from Ref. [67]. Copyright 2020, WILEY-VCH Verlag GmbH & Co. KGaA Publishers. (**B**) Schematic illustration of a fluorescent platform for one-pot rapid identification of fusion gene subtypes based on dimerization of DNA-Ag NCs and fluorescence change, reproduced with permission from Ref. [2]. Copyright 2023, Wiley-VCH Publishers.

### 3.1.5. Other DNA-MNC-Based Nanosystems

In addition to amplification technology, nanomaterials, e.g., upconversion NPs (UC-NPs) and fluorescent nano-aggregators, have been widely applied in DNA-MNC-based analytical methods. A novel biosensor was designed using UCNPs with lanthanide ions (CSUCNPs) and aptamers as recognition elements for the determination of acrylamide (AAm) (Figure 6A) [68]. The DNA three-way junctions consisting of DNA1, DNA2, and AAm aptamer were modified on the silica-coated CSUCNPs (CSUCNPs@SiO2) and acted as the template for producing DNA-Ag NCs. Due to the fluorescence resonance energy transfer (FRET) from CSUCNPs to DNA-Ag NCs, the upconversion emission was quenched by FRET. When AAm was introduced, dissembling of three-way junctions occurred because of binding interaction between AAm and its aptamer and impeded generation of DNA-Ag NCs and FRET, resulting in high fluorescence from CSUCNPs. Our group reported

that Cu NCs exhibited an AIE enhancement effect [90]. Ultra-small Cu NCs with DNA nanoribbons were assembled to improve fluorescence properties of DNA-Cu NCs [69] (Figure 6B). Multiple specific binding sites of DNA nanoribbons served as templates for the in situ synthesis, resulting in enhanced luminescence and excellent fluorescence stability of DNA-Cu NC-based aggregation-induced emission luminogens.
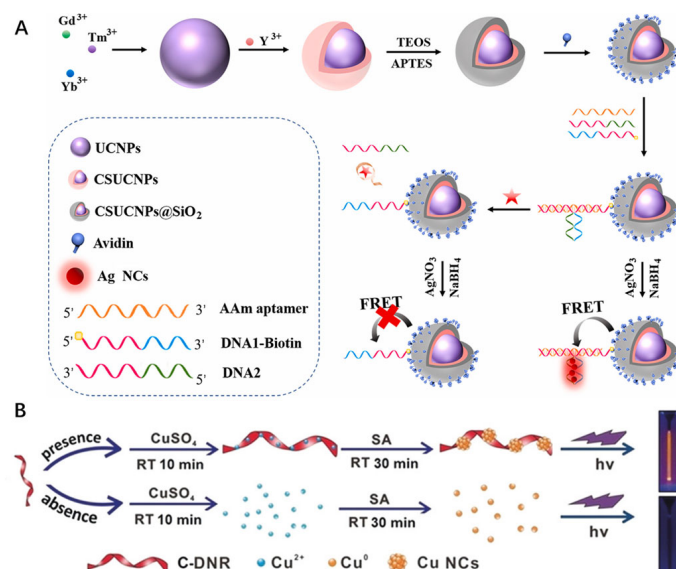


**Figure 6.** (**A**) A scheme illustrating Aam detection based on FRET between SCUCNPs and DNA-Ag NCs, reproduced with permission from Ref. [68]. Copyright 2022, Elsevier B.V. Publishers. (**B**) DNA nanoribbon-guided DNA-Cu NC synthesis and fluorescence improvement, reproduced with permission from Ref. [69]. Copyright 2020, Wiley-VCH Publishers.

### *3.2. Electrochemiluminescence*

Electrochemiluminescence (ECL), also known as electrogenerated chemiluminescence, is a technology that combines electrochemistry and chemiluminescence. ECL is generated by appropriate potential stimulation and has the characteristics of luminescence signal time and potential resolution by controlling the potential. Additionally, in the ECL process, luminophores can be recycled by electrochemical reactions on the electrode surface. Based on the above advantages of low background, high sensitivity, and low detection limit, ECL has attracted much attention from researchers and has been developed as one of the most effective analytical detection methods. The ECL mechanism in the traditional sense is divided into two categories, the self-annihilation path and the co-reaction pathway. The co-reaction pathway overcomes the stability requirements of the self-annihilation path and has become the most widely used strategy. Typical co-reaction systems include tripyridineruthenium ($Ru(by)_3^{2+}$) with tripropylamine (TPA), luminol systems with $H_2O_2$, and quantum dots (QDs) with $K_2S_2O_8$ [91–94]. Since it was first reported that Ag NCs exhibited ECL properties, MNCs (e.g., Ag NCs, Au NCs, and Cu NCs) have been regarded as promising ECL emitters with prominent features of low toxicity and good biocompatibility, as compared to traditional ECL luminophores (e.g., $Ru(by)_3^{2+}$, luminol, and QDs) [95].

### 3.2.1. DNA-MNCs as ECL Luminophores, Resonance Energy Transfer (RET) Acceptors, or Donors

Owing to their advantages of low toxicity, high stability, good water solubility, easy preparation, and biocompatibility, DNA-MNCs are deemed as promising ECL luminophores in bioanalytical methods. For instance, a label-free ECL biosensor for ultrasensitive detection of RNase H activity was developed by using DNA/RNA duplex-templated Cu NCs as novel excellent ECL emitters (Figure 7A) [96]. RNase H can specifically bind to a DNA/RNA duplex, leading to digestion of RNA chains and a decrease in the ECL signal

from Cu NCs. The method exhibited a broad linear range from $3 \times 10^{-3}$ U/mL to 20 U/mL with a detection limit of $1.97 \times 10^{-3}$ U/mL, and satisfactory accuracy in detecting RNase H in human serum indicated great potential for further application in clinical diagnostics. DNA-MNCs can also act as energy acceptors to quench ECL of QDs due to RET between QDs and MNCs. An ECL-RET sensor to achieve effective and sensitive detection of telomerase activity was developed [97]. The specific principle is shown in Figure 7B. The hairpin DNA (H) and telomerase primer were connected to the surface of the CdS QD modified electrode. In the presence of telomerase extract and deoxyribonucleotides (dNTPs), the telomerase primer was extended, and long chains with repeated sequences $(TTAGGG)_n$ that can be hybridized with S DNA were produced. The formation of a DNA walker with multiple S "legs" circularly triggered H cleavage at its specific site by the endonuclease (Nt. BbvCI), and, subsequently, probe-Ag NCs were bound to residual DNA fragments of H and quenched the ECL of CdS QDs on the electrode. The DNA walker as a dynamic DNA nanomachine [98–102] is quite useful in biological analysis due to its excellent mobility and controllability [103]. It should be noted that, unlike traditional single-legged DNA walkers [99,104,105], the multi-legged DNA walker initiated multiple signal responses, thereby shortening walking time and improving signal amplification efficiency.
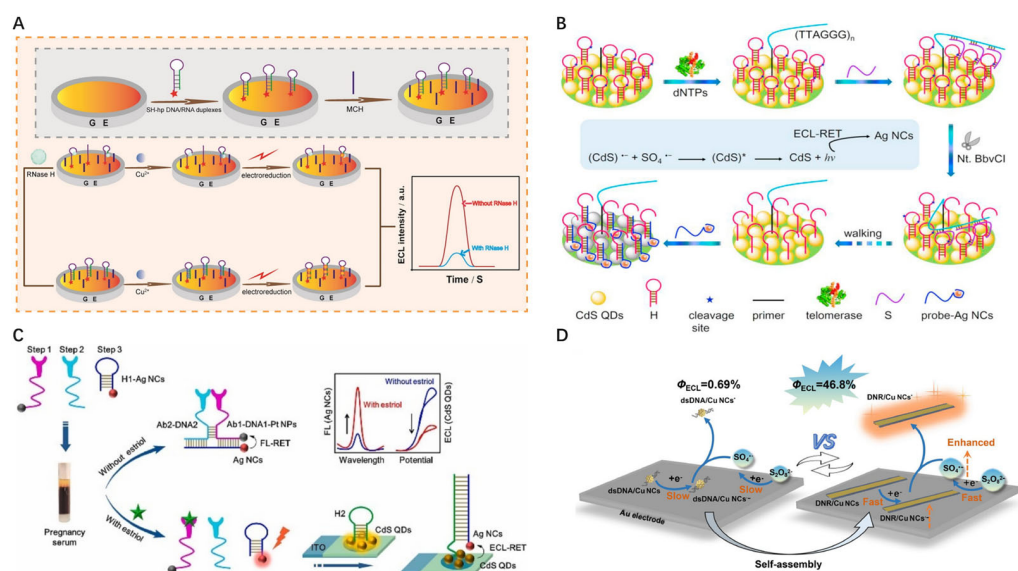


**Figure 7.** (**A**) The principle of a label-free ECL biosensor with DNA-Cu NCs as ELC luminophores for detection of RNaseH activity, the red stars indicate thiol group, reproduced with permission from Ref. [96]. Copyright 2022, Elsevier B.V. Publishers. (**B**) An amplified ECL method for detecting telomerase activity based on DNA walker-triggered ECL-RET between CdS QDs and probe-Ag NCs, reproduced with permission from Ref. [97]. Copyright 2020, Elsevier B.V. Publishers. (**C**) A ratiometric biosensor for sensitive detection of estriol based on the FL-RET between Ag NCs and Pt NPs and ECL-RET between CdS QDs and Ag NCs, reproduced with permission from Ref. [106]. Copyright 2023, Elsevier B.V. Publishers. (**D**) DNA nanoribbon-guided assembling of DNA-MNCs and ECL enhancement, * indicate the excited state of Cu NCs, reproduced with permission from Ref. [3]. Copyright 2023, Wiley-VCH Publishers.

Multi-mode ratiometric methods have been constructed with DNA-MNCs. A two-mode RET-based ratiometric biosensor was designed for highly sensitive detection of estriol [106] (Figure 7C). Both estriol antibody and goat anti-rabbit antibody-labeled DNA probes (Ab1-DNA1-Pt NP and Ab2-DNA2) were hybridized with Ag NCs-labeled DNA strands (H1-AgNCs), and fluorescent RET(FL-RET) between adjacent Ag NCs (donors) and Pt NPs (receptors) caused fluorescence quenching of Ag NCs (FL off). When the target estriol was present and recognized by its antibody Ab1, hybridization between H1-Ag NCs and H2 on CdS QD-loaded ITO led to ECL-RET between Ag NCs and CdS

QDs. Consequently, reverse changes in FL and ECL were observed. The sensor achieves quantification of estriol from 1 to 100 ng/mL.

### 3.2.2. DNA-MNCs as Catalysts for Enhancing ECL

DNA-MNCs can be utilized as catalysts in liquid-phase reactions to enhance ECL emission, improve method sensitivity, and expand the application horizon. Ag NCs using DNA duplexes as templates were prepared and explored the construction of aptamer sensors for the detection of carcinoembryonic antigen (CEA). It was found that Ag NCs and Ag$^+$ stripped from Ag NCs were capable of catalyzing electrochemical reduction and oxidation of $H_2O_2$, respectively, accelerating the decomposition of $H_2O_2$ and producing reactive oxygen species (ROS), thereby effectively intensifying luminol ECL. Combined with Exo-I-assisted cyclic amplification technology, the developed aptamer sensor enabled sensitive detection of CEA, and a wide linear response from 100 ag/mL to 10 ng/mL and a quite low detection limit of 38.86 ag/mL (S/N = 3) were obtained. Programmable DNA nanoribbons were utilized to assemble MNCs (Cu NCs and Au NCs) and enhance ECL activity, since the electron transfer process was improved and the energy gap was decreased because of DNA-induced aggregation [3] (Figure 7D). It was also found that the length, position, and spacing of the DNA template played a key role. This study provides a new avenue for ECL enhancement, but the ECL-enhancing mechanism is not clear.

### 3.3. Antibacterial Activity

MNCs display antibacterial activity via the direct contact reaction of released metal ions (e.g., Ag$^+$) with negatively charged microbial cell membranes, or catalytically generating reactive oxygen species and other free radicals [5,107–110]. The catalytic property of MNCs correlates with various factors, such as size, surface coating, and oxidation state [107]. There have been many reports on DNA-MNCs in the last decade, but only a few have addressed antibacterial activity.

### 3.3.1. Antibacterial Activity of DNA-MNCs and the Mechanism Exploration

Javani and coworkers investigated the antibacterial activity of different DNA-Ag NCs toward positive and negative Gram bacteria and demonstrated that the antibacterial activity was dependent on the sequence of the DNA template [108]. Among these DNA-Ag NCs with different fluorescence emission (i.e., blue, yellow, and red emitters), blue emitters exhibited much lower antibacterial activity, as compared to yellow and red emitters, which is attributed to those complexes with distinct stabilities and structures. Finally, the authors designed a trimeric structure and synthesized the DNA-Ag NCs, which can inhibit the growth of Gram bacteria in the sub-molar range and reveal the highest antibacterial activity. Later, Park et al. reported a novel technique for improving the fluorescence efficiency and stability of DNA-Ag NCs [109]. The particular interaction of melamine with T residues in the DNA template enabled the formation of stable complexes between melamine and DNA-Ag NCs, which revealed intensive fluorescence and superior antibacterial efficacy against Gram bacteria. To the best of our knowledge, this is the first report on DNA-Ag NCs with both improved fluorescence efficiency and effective antibacterial properties.

There are many reports on the use of extremely small Ag NCs for antibacterial purposes, but the antibacterial mechanism has not been fully elucidated. Recent research results on nanostructures containing Ag NCs indicate that information obtained from extended X-ray absorption fine structure (EXAFS) can be used to evaluate the antibacterial activity of Ag NCs [111]. The high antibacterial activity of Ag$_{10}$NC@hpC$_{12}$ (hairpin 12 C) was ascribed to the charged characteristics of Ag NC, its ability for interaction with environmental oxygen, and the production of singlet oxygen [112]. In previous studies, four representative DNA-Ag NCs were investigated. It was concluded that the stability during red fluorescence aging was highly likely a decisive factor for the antibacterial properties of Ag NCs, and a lowered pH was not beneficial to enhance antibacterial activity [113]. The cytotoxicity was also evaluated in the study. When the amount of DNA-Ag NCs was

added to even twice the required concentration to effectively inhibit bacteria, they remained non-toxic to several mammalian cells. Of note, the results also indicated that optical behavior of DNA-Ag NCs may be closely related to the antibacterial properties of these novel nanostructures and would inspire researchers to further explore the antibacterial effects of DNA-Ag NCs on pathogenic and non-pathogenic bacteria.

### 3.3.2. Biocompatibility of Antibacterial DNA-MNCs

Antibacterial nanomaterials hold great potential for treating wounds caused by bacterial infections; however, it is vital to balance their antibacterial activity and biocompatibility. Liu et al. recently employed biocompatible genetic molecule DNA as a building material to prepare antibacterial hydrogel [5]. A Y-DNA nanostructure with three "sticky ends" was constructed from three single-stranded DNA (ssDNA) (Figure 8). A C-rich ring existed at one of the ends and could absorb Ag ions, yielding Y-Ag NCs after reduction by $NaBH_4$. Self-assembly of Y-DNA and Y-Ag via the "sticky ends" led to production of an antibacterial DNA hydrogel. It was validated that both macroscopic and microscopic DNA-Ag complexes can effectively limit bacterial growth in vitro without affecting cell proliferation, and Y-Ag spray may even accelerate wound healing in vivo. The work provides a liable method to develop new wound dressings (such as spray and hydrogel) for therapeutic wound healing.
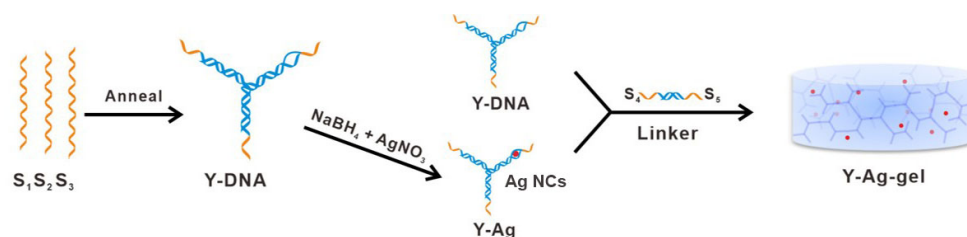


**Figure 8.** Preparation of one antibacterial DNA hydrogel containing DNA-Ag NCs, reproduced with permission from Ref. [5]. Copyright 2022, American Chemical Society Publishers.

### *3.4. Catalysis*

#### 3.4.1. DNA-MNC-Based Nanozymes and Their Analytical Applications

Since $Fe_3O_4$ revealing the properties of natural enzymes was first discovered, many scholars have developed multifarious nanomaterials to simulate natural enzymes (nanozymes) [114]. Nanozymes have many advantages over natural enzymes, such as high stability, low cost, easy synthesis, high efficiency, and recyclability. Peroxidase (POD) is a type of enzyme that uses hydrogen peroxide as an electron acceptor and catalyzes the oxidation of substrates such as phenols and amine compounds, can catalyze oxidation of substrate reagents to generate colored products, and has been widely applied for detection and monitoring of some biological samples [115]. So far, the POD-like aspect of DNA-Ag/Pt NCs has been studied the most.

A simple one-step method for synthesizing DNA-Ag/Pt NCs was developed by Zheng and his colleagues, and highly efficient POD-like catalytic activity was observed [116]. By taking advantage of DNA-Ag/Pt NCs, a label-free colorimetric aptamer sensor was designed using a sandwich strategy for protein detection. The POD-like activity of DNA-Ag/Pt NCs can be inhibited significantly by L-cysteine [117]. Accordingly, a colorimetric method for L-cysteine detection was developed, with a LOD of 2.0 nM and a linear range of 5.0 nM to 500 nM. This low-cost and simple method exhibited high sensitivity and selectivity, which facilitated biological analysis, indicating the excellent analytical application of DNA-Ag/Pt NCs as enzyme mimics.

Based on POD-like activity of DNA-Ag/Pt NCs and in combination with nucleases-assisted DNA amplification, Mu et al. established an amplified colorimetric sensing system for detection of a cancer biomarker (carcinoembryonic antigen, CEA) [118]. As shown in Figure 9, DNA-Ag/Pt NCs can catalyze the oxidation of 3,3,5′,5′-tetramethyl benzidine

(TMB) by $H_2O_2$ to generate blue substance ox-TMB, and by integrating RCA restriction endonuclease (Nb.BbvCl) and CRISPR/Cas12a reactions, CEA can be sensitively determined by naked eyes. In addition to DNA-Ag/Pt NCs, DNA-Cu NCs and DNA-Au NCs also exhibit apparent catalytic activity. Borghei and coworkers reported that DNA (poly T)-Cu NCs with green fluorescence exhibited POD activity comparable to natural enzymes and proposed a colorimetric method for detecting miRNA based on the inhibition of the catalysis toward the oxidation of methylene blue (MB) [119]. A dynamic range of 1.0 pM to 10.0 nM and an ultralow LOD of 0.6 pM were obtained.
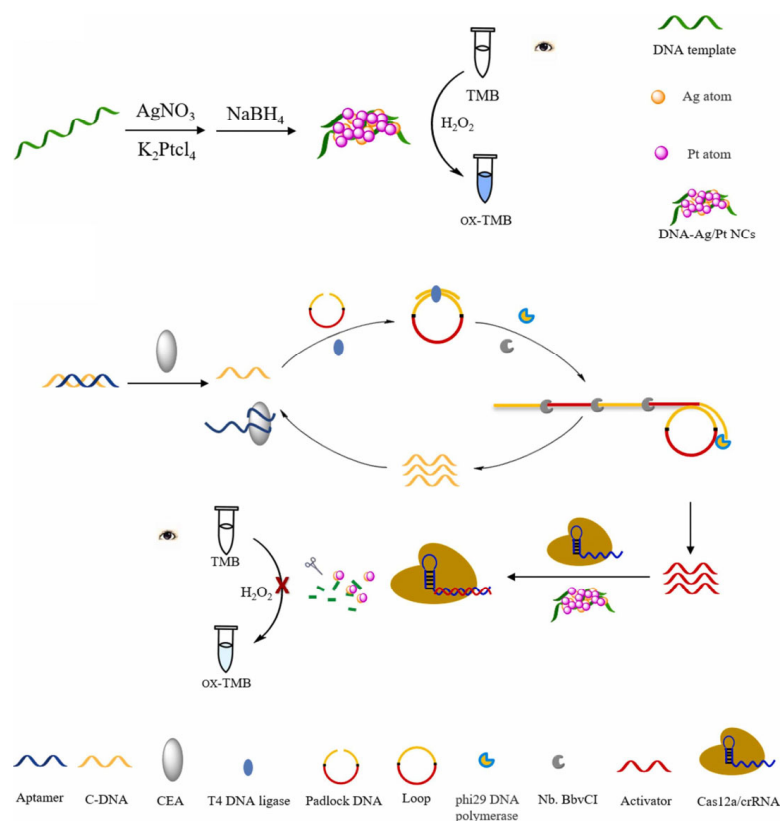


**Figure 9.** A colorimetric and amplified method for CEA detection based on POD-like catalytic activity of DNA-Ag/Pt NCs and nuclease-assisted DNA amplification reactions, reproduced with permission from Ref. [118]. Copyright 2022, Elsevier B.V. Publishers.

DNA-Cu/Ag NCs with C/G-rich DNA as templates (i.e., c-myc TBA-Cu/Ag NC) were synthesized and can emit the strongest and most stable fluorescence emission at approximately 555 nm under neutral and acidic conditions [120] (Figure 10A). Surprisingly, c-myc TBA-Cu/Ag NCs can efficiently and quickly catalyze a TMB-$H_2O_2$ reaction to generate blue ox-TMB under acidic conditions, indicating its high POD-like activity. A colorimetry for glucose analysis was developed with DNA-Cu/Ag NCs with a linear range of 0.1 to 0.7 mM and a LOD of 9.38 μ M and worked in a diluted serum sample, indicating potential application prospects of the DNA-Cu/Ag NC nanozyme. The critical lesson was that C and G bases were capable of improving the catalytic activity of MNCs. Compared with natural enzymes, catalytic activity of most nanozymes is still relatively low. A new method was developed for synthesizing Cu NCs using small molecule nucleosides as templates and hydroxylamine hydrochloride as a reducing agent [121]. After optimizing the catalytic performance of Cu NCs, T-templated Cu NCs (T-Cu NCs) revealed the highest catalytic activity. Based on the interaction between $Hg^{2+}$ and T base, T-Cu NCs were used as nanoprobes for $Hg^{2+}$ detection and displayed excellent selectivity in buffer solutions and actual water samples. These results indicate that nucleosides or DNA provide more possibilities for regulating the enzymatic activity of MNPs. Reaction conditions were sys-

tematically optimized to further expand the application of DNA-Ag NCs as nanocatalysts with 4-nitrophenol (4-NP) reduction as a model reaction and revealed their potential for boosting degradation of a series of nitrobenzene derivatives in industry [122]. It was found that DNA-Ag NCs maintained their catalytic activity even at the high temperature of close to 100 °C, which drastically expanded their application scope.
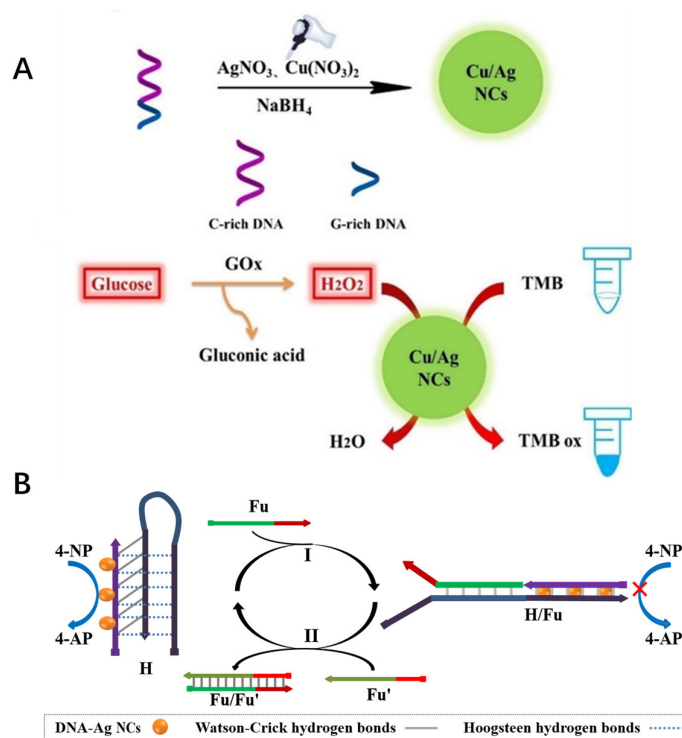


**Figure 10.** (**A**) Preparation of DNA-Cu/Ag NCs with a C/G-rich DNA sequence and their application for glucose based on POD-like catalytic activity, reproduced with permission from Ref. [120]. Copyright 2020, Wiley-VCH Verlag GmbH & Co. KGaA Publishers. (**B**) Reversible regulation of catalytic activity of DNA-Ag NCs based on their differential interactions with DNA structures and stimuli-responsive structural transition, reproduced with permission from Ref. [4]. Copyright 2020, Wiley-VCH GmbH Publishers.

### 3.4.2. Regulating Catalytic Activities of DNA-MNCs for Analysis and Logic Operation

Nanomaterial-based catalysts possess prominent robust and low-cost merits, but the uncontrollable drawbacks seriously affect their applications in the field of biomedicine. A large number of editable nucleic acid molecules not only can serve as ligands for synthesis and stabilization of nanomaterials but also provide a good material foundation for regulating the properties of nanomaterials, especially in the controllability and applicability of catalytic activity. The research on biomimetic catalytic materials based on nucleic acid/nanocomposite systems is still in the infant stage. Our group achieved reversible regulation of catalytic activity of DNA-Ag NCs with DNA systems (Figure 10B) [4]. Four DNA homopolymers (poly A, poly G, poly C, and poly T) and secondary structures (d(AT) duplex and d(TAT) triplex) exhibited distinct inhibition effects on the catalytic activity of DNA-Ag NCs, namely, poly A > poly G > poly C > poly T, and poly A ≈ d(AT) >> d(TAT). It was disclosed that N7 groups of A bases were involved in DNA binding to DNA-Ag NCs and blocking of active sites. Based on the inhibition effects and reversible transformation between duplexes and triplexes, an allosteric hairpin DNA (H) was designed, which can undergo structural transition and alter the catalytic activity of absorbed DNA-Ag NCs under stimulation of fuel strands (Fu and Fu'). Concomitantly, two low-cost and convenient biosensing methods were obtained, based on the switchable platform. It is worth looking forward to the hope that DNA-Ag NCs with controlled catalysis will courage researchers

to design multifunctional nanocatalysts and contribute to future intelligent biomedicine. A series of molecular logic gates, including YES, OR, INHIBIT, XOR, and MAJORITY, have also been proposed, which can logically control the catalytic activity of DNA-Ag NCs [123]. Unlike most DNA-Ag NC-based logic gates in the past, the catalytic effect was used as an output signal rather than variable fluorescence, providing a novel and robust strategy for fabricating molecular logic gates. Additionally, by virtue of programmable DNA reactions and specific recognition of aptamers, intelligent detection of cardiac biomarkers was realized.

### 3.4.3. DNA-MNCs as Nanocatalysts in the Field of Energy Source

The catalysis of MNCs not only has been utilized for sensing and logic systems but also can be applied in the field of energy sources. The research on exploring effective nanocatalysts to split water into hydrogen and oxygen has advanced significantly in recent years. The water decomposition efficiency has increased from about 1% to over 10% with the emergence of multifarious nanocatalysts, and Jennifer et al. demonstrated that DNA-Au NCs were able to promote electron transfer (ET) in enzymatic electroreduction processes [124]. A novel DNA-Au NC with a diameter of roughly 1 nm and approximately 7 Au atoms was prepared. Coupled with bilirubin oxidase (BOD) and single wall carbon nanotubes (SWNT), the DNA-Au NCs can act as an ET promoter, lower the overpotential of electrocatalytic oxygen reduction reaction (ORR) by about 15 mV, and improve the electrocatalytic current density. The Yang group recently reported that ssDNA-templated Cu NCs can be employed for electrocatalytic production of $NH_3$ [125], since ssDNA conduced to promote production on the electrode via water distribution optimization and hydrogen bonding network connectivity. A high yield of $NH_3$ (2.62 mg·h$^{-1}$·cm$^{-2}$) was obtained.

## 4. Conclusions and Perspectives

DNA-MNCs, e.g., DNA-Ag NCs, DNA-Cu NCs, DNA-Au NCs, and DNA-Ag/Pt NCs, have attracted wide attention in recent years, owing to their prominent properties, e.g., fluorescence, ECL, antibacterial, and catalytic activity, and have been applied in various fields, such as biosensors, logic operation, antibacterial, and energy catalysis. In this review, the synthetic methods for DNA-MNCs are first simply introduced, and then their applications owing to diverse properties are presented and intriguing features of lasted research are emphasized.

(1) DNA-MNCs, particularly DNA-Ag NCs and DNA-Cu NCs, have obvious fluorescence emission, which correlates with the sequences and structures of DNA templates. Varieties of novel biosensing systems have been constructed based on fluorescence regulation, e.g., enhancement by adjacent G-rich sequences, emission alteration by formation of dimeric structures, etc. Many amplification strategies including nuclease-assisted DNA reactions (e.g., RCA and LAMP) and enzyme-free DNA circuits (e.g., CHA and HCR) have been extensively adopted with fluorescent DNA-MNCs for sensitive bioanalysis.

(2) DNA-MNCs as effective ECL emitters can substitute for classical ECL luminophores and have been utilized especially for construction of sensitive analytical methods. DNA-MNCs are able to quench the ECL of luminophores or act as catalysts to intensify the ECL and have been used in biosensing systems. Therefore, DNA-MNCs in ECL systems may play more than one role, and underlying mechanisms need to be further resolved. DNA-Ag NCs exhibit apparent antibacterial activity, and it has been suggested that a correlation exists between fluorescence and antibacterial properties of DNA-Ag NCs.

(3) DNA-MNCs, e.g., DNA-Ag NCs, DNA-Ag/Pt NCs, and DNA-Cu/Ag NCs, as intriguing nanocatalysts, exhibit apparent catalytic activity toward different reactions, such as POD-like activity (nanozyme), nitrobenzene reduction, ORR, etc. Based on the catalytic activity of DNA-MNCs instead of natural enzymes, many robust colorimetric sensing systems have been fabricated. Of note, successful reversible regulation of

catalytic activity of DNA-Ag NCs with DNA systems predicts the potential to explore controllable nanocatalysts.

DNA-MNCs, as one type of DNA-encoded nanomaterials, have been studied extensively in recent years, and much attractive progress has been obtained. Meanwhile, much more effort needs to be devoted to those challenges, as follows.

(1) The relationship between structures and properties has not been resolved and should be attended to. It is anticipated that more precise atomic structures of DNA-MNCs can be acquired with multifarious advanced techniques in the future so as to interpret the underlying mechanisms of properties of DNA-MNCs well and spur their applications in various fields.

(2) DNA-MNCs in ECL systems may play significant roles, such as luminophores, catalysts, or quenchers. It is critical to synthesize well-dispersed MNCs and high ECL activity and expand their potential applications.

(3) Much more comprehensive research is required on the relationship between the antibacterial properties and fluorescence of DNA-MNC. DNA-MNCs can be modified with specific antibodies or aptamers to improve antibacterial targeting, and other antibacterial molecules with different sterilization mechanisms can be employed to augment their antibacterial effects.

(4) There are many types of natural enzymes, and in the future, it is necessary to design and develop DNA-MNCs with new catalytic properties. DNA-MNCs lack specificity and cannot catalyze a specific substrate like natural enzymes, and how to endow DNA-MNCs with specific functions will be a major challenge. It is essential to strengthen the combined application of DNA-MNCs with other technologies.

Taken together, due to their prominent merits, e.g., inherent stability, low production cost, controllable and multifarious properties, etc., DNA-MNCs are expected to be applied in various fields, such as small molecule sensing, environmental governance, disease diagnosis and treatment, and so on.

**Author Contributions:** Conceptualization, J.R. and E.W.; data collection, F.Y., J.R. and E.W.; writing—original draft preparation, F.Y. and J.R.; writing—review and editing, F.Y., J.R. and E.W.; supervision, J.R. and E.W. All authors have read and agreed to the published version of the manuscript.

**Data Availability Statement:** Not applicable.

**Conflicts of Interest:** The authors declare no conflict of interest.

## References

1. Xu, F.; Qing, T.; Qing, Z. DNA-Coded Metal Nano-Fluorophores: Preparation, Properties and Applications in Biosensing and Bioimaging. *Nano Today* **2021**, *36*, 101021. [CrossRef]
2. Gou, X.L.; Zhang, Y.L.; Zhu, S.S.; Yu, X.L.; Qin, L.; Cheng, X.X.; Zhang, Y.H.; Ding, S.J.; Chen, R.; Tang, H.; et al. Asymmetric Hairpins DNA Encapsulated Silver Nanoclusters for in Situ Fluorescence Imaging of Fusion Gene Isoforms in Bone Marrow. *Small* **2023**, *19*, 2303034. [CrossRef] [PubMed]
3. Ouyang, X.; Wu, Y.; Guo, L.; Li, L.; Zhou, M.; Li, X.; Liu, T.; Ding, Y.; Bu, H.; Xie, G.; et al. Self-Assembly Induced Enhanced Electrochemiluminescence of Copper Nanoclusters Using DNA Nanoribbon Templates. *Angew. Chem.-Int. Ed.* **2023**, *62*, e2023008. [CrossRef] [PubMed]
4. Guo, Y.; Lv, M.; Ren, J.; Wang, E. Regulating Catalytic Activity of DNA-Templated Silver Nanoclusters Based on Their Differential Interactions with DNA Structures and Stimuli-Responsive Structural Transition. *Small* **2021**, *17*, 2006553. [CrossRef]
5. Liu, S.; Yan, Q.; Cao, S.; Wang, L.; Luo, S.-H.; Lv, M. Inhibition of Bacteria in Vitro and in Vivo by Self-Assembled DNA-Silver Nanocluster Structures. *ACS Appl. Mater. Interfaces* **2022**, *14*, 41809–41818. [CrossRef] [PubMed]
6. Fan, D.Q.; Wang, J.; Wang, E.K.; Dong, S.J. Propelling DNA Computing with Materials' Power: Recent Advancements in Innovative DNA Logic Computing Systems and Smart Bio-Applications. *Adv. Sci.* **2020**, *7*, 2001766. [CrossRef] [PubMed]
7. Xu, J.; Zhu, X.; Zhou, X.; Khusbu, F.Y.; Ma, C. Recent Advances in the Bioanalytical and Biomedical Applications of DNA-Templated Silver Nanoclusters. *TrAC-Trends Anal. Chem.* **2020**, *124*, 115786. [CrossRef]

8. Cerretani, C.; Liisberg, M.B.; Ruck, V.; Kondo, J.; Vosch, T. The Effect of Inosine on the Spectroscopic Properties and Crystal Structure of a Nir-Emitting DNA-Stabilized Silver Nanocluster. *Nanoscale Adv.* **2022**, *4*, 3212–3217. [CrossRef] [PubMed]

9. Wong, Z.W.; Muthoosamy, K.; Mohamed, N.A.H.; New, S.Y. A Ratiometric Fluorescent Biosensor Based on Magnetic-Assisted Hybridization Chain Reaction and DNA-Templated Silver Nanoclusters for Sensitive Microrna Detection. *Biosens. Bioelectron. X* **2022**, *12*, 100244. [CrossRef]

10. Qing, T.; Zhang, K.; Qing, Z.; Wang, X.; Long, C.; Zhang, P.; Hu, H.; Feng, B. Recent Progress in Copper Nanocluster-Based Fluorescent Probing: A Review. *Microchim. Acta* **2019**, *186*, 670. [CrossRef]

11. Zhang, Q.; Yang, M.; Zhu, Y.; Mao, C. Metallic Nanoclusters for Cancer Imaging and Therapy. *Curr. Med. Chem.* **2018**, *25*, 1379–1396. [CrossRef]

12. Saheb, A.; Smith, J.A.; Josowicz, M.; Janata, J.; Baer, D.R.; Engelhard, M.H. Controlling Size of Gold Clusters in Polyaniline from Top-Down and from Bottom-Up. *J. Electroanal. Chem.* **2008**, *621*, 238–244. [CrossRef]

13. Muhammed, M.A.H.; Ramesh, S.; Sinha, S.S.; Pal, S.K.; Pradeep, T. Two Distinct Fluorescent Quantum Clusters of Gold Starting from Metallic Nanoparticles by Ph-Dependent Ligand Etching. *Nano Res.* **2008**, *1*, 333–340. [CrossRef]

14. Chen, L.; Gharib, M.; Zeng, Y.; Roy, S.; Nandi, C.K.; Chakraborty, I. Advances in Bovine Serum Albumin-Protected Gold Nanoclusters: From Understanding the Formation Mechanisms to Biological Applications. *Mater. Today Chem.* **2023**, *29*, 101460. [CrossRef]

15. Li, Q.; Huang, B.; Yang, S.; Zhang, H.; Chai, J.; Pei, Y.; Zhu, M. Unraveling the Nucleation Process from a Au(I)-Sr Complex to Transition-Size Nanoclusters. *J. Am. Chem. Soc.* **2021**, *143*, 15224–15232. [CrossRef] [PubMed]

16. Brust, M.; Walker, M.; Bethell, D.; Schiffrin, D.J.; Whyman, R. Synthesis of Thiol-Derivatised Gold Nanoparticles in a Two-Phase Liquid–Liquid System. *J. Chem. Soc. Chem. Commun.* **1994**, *7*, 801–802. [CrossRef]

17. Petty, J.T.; Zheng, J.; Hud, N.V.; Dickson, R.M. DNA-Templated Ag Nanocluster Formation. *J. Am. Chem. Soc.* **2004**, *126*, 5207–5212. [CrossRef]

18. Qing, Z.; He, X.; He, D.; Wang, K.; Xu, F.; Qing, T.; Yang, X. Poly(Thymine)-Templated Selective Formation of Fluorescent Copper Nanoparticles. *Angew. Chem.-Int. Ed.* **2013**, *52*, 9719–9722. [CrossRef]

19. Liu, G.; Shao, Y.; Ma, K.; Cui, Q.; Wu, F.; Xu, S. Synthesis of DNA-Templated Fluorescent Gold Nanoclusters. *Gold Bull.* **2012**, *45*, 69–74. [CrossRef]

20. Peyser, L.A.; Vinson, A.E.; Bartko, A.P.; Dickson, R.M. Photoactivated Fluorescence from Individual Silver Nanoclusters. *Science* **2001**, *291*, 103–106. [CrossRef]

21. Zhang, H.; Huang, X.; Li, L.; Zhang, G.; Hussain, I.; Li, Z.; Tan, B. Photoreductive Synthesis of Water-Soluble Fluorescent Metal Nanoclusters. *Chem. Commun.* **2012**, *48*, 567–569. [CrossRef] [PubMed]

22. Liu, Y.-F.; Wang, G.-Q.; Zhao, J.-B.; Jiang, L.; Fang, S.-M.; Sun, Y.-A. Synthesis of Chiral Silver Nanoclusters Capped with Small Molecules. *Colloid Surf. A-Physicochem. Eng. Asp.* **2013**, *426*, 12–17. [CrossRef]

23. Fujimura, T.; Yoshida, Y.; Inoue, H.; Shimada, T.; Takagi, S. Dense Deposition of Gold Nanoclusters Utilizing a Porphyrin/Inorganic Layered Material Complex as the Template. *Langmuir* **2015**, *31*, 9142–9147. [CrossRef] [PubMed]

24. Reetz, M.T.; Helbig, W. Size-Selective Synthesis of Nanostructured Transition. *J. Am. Chem. Soc.* **1994**, *116*, 7401–7402. [CrossRef]

25. Vilar-Vidal, N.; Blanco, M.C.; Lopez-Quintela, M.A.; Rivas, J.; Serra, C. Electrochemical Synthesis of Very Stable Photoluminescent Copper Clusters. *J. Phys. Chem. C* **2010**, *114*, 15924–15930. [CrossRef]

26. Xu, Y.; Chen, Y.; Yang, N.; Sun, L.; Li, G. DNA-Templated Silver Nanoclusters Formation at Gold Electrode Surface and Its Application to Hydrogen Peroxide Detection. *Chin. J. Chem.* **2012**, *30*, 1962–1965. [CrossRef]

27. Kang, J.; Gao, P.; Zhang, G.; Shi, L.; Zhou, Y.; Wu, J.; Shuang, S.; Zhang, Y. Rapid Sonochemical Synthesis of Copper Nanoclusters with Red Fluorescence for Highly Sensitive Detection of Silver Ions. *Microchem. J.* **2022**, *178*, 107370. [CrossRef]

28. Xu, H.; Suslick, K.S. Sonochemical Synthesis of Highly Fluorescent Ag Nanoclusters. *ACS Nano* **2010**, *4*, 3209–3214. [CrossRef]

29. Harshita; Park, T.-J.; Kailasa, S.K. Microwave-Assisted Synthesis of Blue Fluorescent Molybdenum Nanoclusters with Maltose-Cysteine Schiff Base for Detection of Myoglobin and Γ-Aminobutyric Acid in Biofluids. *Luminescence* **2023**, *38*, 1374–1384. [CrossRef]

30. Manno, R.; Ranjan, P.; Sebastian, V.; Mallada, R.; Irusta, S.; Sharma, U.K.; Van der Eycken, E.V.; Santamaria, J. Continuous Microwave-Assisted Synthesis of Silver Nanoclusters Confined in Mesoporous Sba-15: Application in Alkyne Cyclizations. *Chem. Mat.* **2020**, *32*, 2874–2883. [CrossRef]

31. Shang, L.; Dong, S.; Nienhaus, G.U. Ultra-Small Fluorescent Metal Nanoclusters: Synthesis and Biological Applications. *Nano Today* **2011**, *6*, 401–418. [CrossRef]

32. Wang, B.; Zhao, M.; Mehdi, M.; Wang, G.; Gao, P.; Zhang, K.-Q. Biomolecule-Assisted Synthesis and Functionality of Metal Nanoclusters for Biological Sensing: A Review. *Mat. Chem. Front.* **2019**, *3*, 1722–1735. [CrossRef]

33. Borse, S.; Murthy, Z.V.P.; Park, T.J.; Kailasa, S.K. The Influence of Surface Ligand Chemistry for the Synthesis of Blue Fluorescent Gold Nanoclusters for the Detection of Serotonin in Biofluids. *New J. Chem.* **2023**, *47*, 3075–3083. [CrossRef]

34. Zhang, X.; Qian, Y.; Ma, X.; Xia, M.; Li, S.; Zhang, Y. Thiolated DNA-Templated Silver Nanoclusters with Strong Fluorescence Emission and a Long Shelf-Life. *Nanoscale* **2018**, *10*, 76–81. [CrossRef] [PubMed]

35. Yang, X.; Gan, L.; Han, L.; Wang, E.; Wang, J. High-Yield Synthesis of Silver Nanoclusters Protected by DNA Monomers and Dft Prediction of Their Photoluminescence Properties. *Angew. Chem.-Int. Ed.* **2013**, *52*, 2022–2026. [CrossRef]

36. Li, W.; Liu, L.; Fu, Y.; Sun, Y.; Zhang, J.; Zhang, R. Effects of Polymorphic DNA on the Fluorescent Properties of Silver Nanoclusters. *Photochem. Photobiol. Sci.* **2013**, *12*, 1864–1872. [CrossRef]
37. Teng, Y.; Jia, X.; Zhang, S.; Zhu, J.; Wang, E. A Nanocluster Beacon Based on the Template Transformation of DNA-Templated Silver Nanoclusters. *Chem. Commun.* **2016**, *52*, 1721–1724. [CrossRef]
38. Rotaru, A.; Dutta, S.; Jentzsch, E.; Gothelf, K.; Mokhir, A. Selective Dsdna-Templated Formation of Copper Nanoparticles in Solution. *Angew. Chem.-Int. Ed.* **2010**, *49*, 5665–5667. [CrossRef]
39. Liu, G.; Shao, Y.; Peng, J.; Dai, W.; Liu, L.; Xu, S.; Wu, F.; Wu, X. Highly Thymine-Dependent Formation of Fluorescent Copper Nanoparticles Templated by Ss-DNA. *Nanotechnology* **2013**, *24*, 345502. [CrossRef]
40. Deng, H.-H.; Wang, F.-F.; Shi, X.-Q.; Peng, H.-P.; Liu, A.-L.; Xia, X.-H.; Chen, W. Water-Soluble Gold Nanoclusters Prepared by Protein-Ligand Interaction as Fluorescent Probe for Real-Time Assay of Pyrophosphatase Activity. *Biosens. Bioelectron.* **2016**, *83*, 1–8. [CrossRef]
41. Liu, J.; Yu, M.; Zhou, C.; Yang, S.; Ning, X.; Zheng, J. Passive Tumor Targeting of Renal-Clearable Luminescent Gold Nanoparticles: Long Tumor Retention and Fast Normal Tissue Clearance. *J. Am. Chem. Soc.* **2013**, *135*, 4978–4981. [CrossRef]
42. Shu, T.; Su, L.; Wang, J.; Lu, X.; Liang, F.; Li, C.; Zhang, X. Value of the Debris of Reduction Sculpture: Thiol Etching of Au Nanoclusters for Preparing Water-Soluble and Aggregation-Induced Emission-Active Au(I) Complexes as Phosphorescent Copper Ion Sensor. *Anal. Chem.* **2016**, *88*, 6071–6077. [CrossRef]
43. Wu, X.; Zhang, Z.; Li, J.; You, H.; Li, Y.; Chen, L. Molecularly Imprinted Polymers-Coated Gold Nanoclusters for Fluorescent Detection of Bisphenol A. *Sens. Actuator B-Chem.* **2015**, *211*, 507–514. [CrossRef]
44. Almowalad, J.; Laskar, P.; Somani, S.; Meewan, J.; Tate, R.J.; Dufes, C. Lactoferrin- and Dendrimer-Bearing Gold Nanocages for Stimulus-Free DNA Delivery to Prostate Cancer Cells. *Int. J. Nanomed.* **2022**, *17*, 1409–1421. [CrossRef]
45. Kawasaki, H.; Hamaguchi, K.; Osaka, I.; Arakawa, R. Ph-Dependent Synthesis of Pepsin-Mediated Gold Nanoclusters with Blue Green and Red Fluorescent Emission. *Adv. Funct. Mater.* **2011**, *21*, 3508–3515. [CrossRef]
46. Rao, T.U.B.; Pradeep, T. Luminescent Ag-7 and Ag-8 Clusters by Interfacial Synthesis. *Angew. Chem.-Int. Ed.* **2010**, *49*, 3925–3929.
47. Cao, Y.T.; Fung, V.; Yao, Q.F.; Chen, T.K.; Zang, S.Q.; Jiang, D.E.; Xie, J.P. Control of Single-Ligand Chemistry on Thiolated Au-25 Nanoclusters. *Nat. Commun.* **2020**, *11*, 5498. [CrossRef] [PubMed]
48. Cao, Y.; Liu, T.; Chen, T.; Zhang, B.; Jiang, D.-e.; Xie, J. Revealing the Etching Process of Water-Soluble Au-25 Nanoclusters at the Molecular Level. *Nat. Commun.* **2021**, *12*, 3212. [CrossRef]
49. Braun, E.; Eichen, Y.; Sivan, U.; Ben-Yoseph, G. DNA-Templated Assembly and Electrode Attachment of a Conducting Silver Wire. *Nature* **1998**, *391*, 775–778. [CrossRef] [PubMed]
50. Arakawa, H.; Neault, J.F.; Tajmir-Riahi, H.A. Silver(I) Complexes with DNA and Rna Studied by Fourier Transform Infrared Spectroscopy and Capillary Electrophoresis. *Biophys. J.* **2001**, *81*, 1580–1587. [CrossRef] [PubMed]
51. Berti, L.; Burley, G.A. Nucleic Acid and Nucleotide-Mediated Synthesis of Inorganic Nanoparticles. *Nat. Nanotechnol.* **2008**, *3*, 81–87. [CrossRef]
52. Noguera, M.; Bertran, J.; Sodupe, M. $Cu^{2+/+}$ Cation Coordination to Adenine-Thymine Base Pair. Effects on Intermolecular Proton-Transfer Processes. *J. Phys. Chem. B* **2008**, *112*, 4817–4825. [CrossRef] [PubMed]
53. Gibson, D.W.; Beer, M.; Barrnett, R.J. Gold (Iii) Complexes of Adenine Nucleotides. *Biochemistry* **1971**, *10*, 3669–3679. [CrossRef]
54. Kennedy, T.A.C.; MacLean, J.L.; Liu, J. Blue Emitting Gold Nanoclusters Templated by Poly-Cytosine DNA at Low Ph and Poly-Adenine DNA at Neutral Ph. *Chem. Commun.* **2012**, *48*, 6845–6847. [CrossRef] [PubMed]
55. Guo, W.; Yuan, J.; Dong, Q.; Wang, E. Highly Sequence-Dependent Formation of Fluorescent Silver Nanoclusters in Hybridized DNA Duplexes for Single Nucleotide Mutation Identification. *J. Am. Chem. Soc.* **2010**, *132*, 932–934. [CrossRef]
56. Ritchie, C.M.; Johnsen, K.R.; Kiser, J.R.; Antoku, Y.; Dickson, R.M.; Petty, J.T. Ag Nanocluster Formation Using a Cytosine Oligonucleotide Template. *J. Phys. Chem. C* **2007**, *111*, 175–181. [CrossRef] [PubMed]
57. Han, B.; Wang, E. DNA-Templated Fluorescent Silver Nanoclusters. *Anal. Bioanal. Chem.* **2012**, *402*, 129–138. [CrossRef]
58. Kailasa, S.K.; Borse, S.; Koduru, J.R.; Murthy, Z.V.P. Biomolecules as Promising Ligands in the Synthesis of Metal Nanoclusters: Sensing, Bioimaging and Catalytic Applications. *Trends Environ. Anal. Chem.* **2021**, *32*, e00140. [CrossRef]
59. Zhao, Z.; Li, Y. Developing Fluorescent Copper Nanoclusters: Synthesis, Properties, and Applications. *Colloids Surf. B-Biointerfaces* **2020**, *195*, 111244. [CrossRef]
60. Han, S.; Zhang, Z.; Li, S.; Qi, L.; Xu, G. Chemiluminescence and Electrochemiluminescence Applications of Metal Nanoclusters. *Sci. China-Chem.* **2016**, *59*, 794–801. [CrossRef]
61. Qin, L.; Zhang, K.; Feng, B.; Zhang, P.; Qing, T.; Fei, J. Proximity Sequence-Dependent Spectral Conversion of Silver Nanoclusters and Construction of Ratiometric Nanoprobe. *Chem. Eng. J.* **2022**, *441*, 136001. [CrossRef]
62. Chen, N.; Gong, C.; Zhao, H. Dual-Channel Fluorescence Detection of Antibiotic Resistance Genes Based on DNA-Templated Silver Nanoclusters. *Sci. Total Environ.* **2023**, *882*, 163559. [CrossRef]
63. Shi, H.; Bi, X.; Zhang, J.; Duan, S.; Yan, J.; Jia, H. Simple and Sensitive Detection of Microrna Based on Guanine-Rich DNA-Enhanced Fluorescence of DNA-Templated Silver Clusters. *Talanta* **2023**, *253*, 124065. [CrossRef]
64. Ma, L.; Wang, J.; Li, Y.; Liao, D.; Zhang, W.; Han, X.; Man, S. A Ratiometric Fluorescent Biosensing Platform for Ultrasensitive Detection of Salmonella Typhimurium Via Crispr/Cas12a and Silver Nanoclusters. *J. Hazard. Mater.* **2023**, *443*, 130234. [CrossRef] [PubMed]

65. Zhou, Y.; Zeng, Y.; Zhang, D.; Qi, P.; Wang, Y.; Xin, Y.; Sun, Y. Bacterial DNA Analysis Based on Target Aided Self-Assembly Cycle Amplification Coupled with DNA-Agncs/Three-Way DNA Junction. *Sens. Actuator B-Chem.* **2023**, *374*, 132749. [CrossRef]

66. Yang, M.; Li, H.; Li, X.; Huang, K.; Xu, W.; Zhu, L. Catalytic Hairpin Self-Assembly Regulated Chameleon Silver Nanoclusters for the Ratiometric Detection of Circrna. *Biosens. Bioelectron.* **2022**, *209*, 114258. [CrossRef]

67. Lv, M.; Zhou, W.; Fan, D.; Guo, Y.; Zhu, X.; Ren, J.; Wang, E. Illuminating Diverse Concomitant DNA Logic Gates and Concatenated Circuits with Hairpin DNA-Templated Silver Nanoclusters as Universal Dual-Output Generators. *Adv. Mater.* **2020**, *32*, 1908480. [CrossRef]

68. Rong, Y.; Hassan, M.M.; Ouyang, Q.; Zhang, Y.; Wang, L.; Chen, Q. An Upconversion Biosensor Based on DNA Hybridization and DNA-Templated Silver Nanoclusters for the Determination of Acrylamide. *Biosens. Bioelectron.* **2022**, *215*, 114581. [CrossRef] [PubMed]

69. Ouyang, X.; Wang, M.; Guo, L.; Cui, C.; Liu, T.; Ren, Y.; Zhao, Y.; Ge, Z.; Guo, X.; Xie, G.; et al. DNA Nanoribbon-Templated Self-Assembly of Ultrasmall Fluorescent Copper Nanoclusters with Enhanced Luminescence. *Angew. Chem.-Int. Ed.* **2020**, *59*, 11836–11844. [CrossRef] [PubMed]

70. Shao, X.; Zhu, L.; Zhang, Y.; Du, Z.; Sun, C.; Xu, W. Integration of Ion-Tuned Oligonucleotide Structural Motifs and DNA-Templated Copper Nanoclusters as a Manipulable Logic Device. *Sens. Actuator B-Chem.* **2020**, *325*, 128769. [CrossRef]

71. Yang Qing, H.F.; Yang, Y.; Liao, Y.; Li, H.; Wang, Z.; Du, J. Enzyme-Assisted Amplification and Copper Nanocluster Fluorescence Signal-Based Method for Mirna-122 Detection. *Biosensors* **2023**, *13*, 854. [CrossRef]

72. Li, J.; Zhang, M.; Wang, H.; Wu, J.; Zheng, R.; Zhang, J.; Li, Y.; Wang, Z.; Dai, Z. Sensitive Determination of Formamidopyrimidine DNA Glucosylase Based on Phosphate Group-Modulated Multi-Enzyme Catalysis and Fluorescent Copper Nanoclusters. *Analyst* **2020**, *145*, 5174–5179. [CrossRef]

73. Chen, C.-A.; Wang, C.-C.; Kou, H.-S.; Wu, S.-M. Molecular Inversion Probe-Rolling Circle Amplification with Single-Strand Poly-T Luminescent Copper Nanoclusters for Fluorescent Detection of Single-Nucleotide Variant of Smn Gene in Diagnosis of Spinal Muscular Atrophy. *Anal. Chim. Acta* **2020**, *1123*, 56–63. [CrossRef] [PubMed]

74. Tao, Y.; Yi, K.; Wang, H.; Li, K.; Li, M. Metal Nanoclusters Combined with Crispr-Cas12a for Hepatitis B Virus DNA Detection. *Sens. Actuator B-Chem.* **2022**, *361*, 131711. [CrossRef]

75. Wu, N.-N.; Chen, L.-G.; Xiao, M.-Z.; Yuan, R.-Y.; Wang, H.-B. Determination of Trypsin Using Protamine Mediated Fluorescent Enhancement of DNA Templated Au Nanoclusters. *Microchim. Acta* **2023**, *190*, 158. [CrossRef] [PubMed]

76. Teng, Y.; Yang, X.; Han, L.; Wang, E. The Relationship between DNA Sequences and Oligonucleotide-Templated Silver Nanoclusters and Their Fluorescence Properties. *Chem. Eur. J.* **2014**, *20*, 1111–1115. [CrossRef]

77. Li, T.; Zhang, L.B.; Ai, J.; Dong, S.J.; Wang, E.K. Ion-Tuned DNA/Ag Fluorescent Nanoclusters as Versatile Logic Device. *ACS Nano* **2011**, *5*, 6334–6338. [CrossRef]

78. Xu, M.; Wang, X.; Tian, J.; Chen, J.; Wei, X.; Li, W. A Clamp-Improved Universal Amplified System for Ratiometric Fluorescent Detection of Single-Nucleotide Polymorphisms Coupled with a Novel Dual-Emissive Silver Nanocluster. *Sens. Actuator B-Chem.* **2022**, *367*, 132151. [CrossRef]

79. Guo, W.W.; Yuan, J.P.; Wang, E.K. Strand Exchange Reaction Modulated Fluorescence "Off-On" Switching of Hybridized DNA Duplex Stabilized Silver Nanoclusters. *Chem. Commun.* **2011**, *47*, 10930–10932. [CrossRef] [PubMed]

80. Cao, Q.; Teng, Y.; Yang, X.; Wang, J.; Wang, E. A Label-Free Fluorescent Molecular Beacon Based on DNA-Ag Nanoclusters for the Construction of Versatile Biosensors. *Biosens. Bioelectron.* **2015**, *74*, 318–321. [CrossRef]

81. Dadmehr, M.; Hosseini, M.; Hosseinkhani, S.; Ganjali, M.R.; Sheikhnejad, R. Label Free Colorimetric and Fluorimetric Direct Detection of Methylated DNA Based on Silver Nanoclusters for Cancer Early Diagnosis. *Biosens. Bioelectron.* **2015**, *73*, 108–113. [CrossRef]

82. Wang, R.L.; Lan, L.; Liu, L.; Cheng, L. Asymmetric Polymerase Chain Reaction and Loop-Mediated Isothermal Amplification (Ap-Lamp) for Ultrasensitive Detection of Micrornas. *Chin. Chem. Lett.* **2020**, *31*, 159–162. [CrossRef]

83. Tian, W.M.; Li, P.J.; He, W.L.; Liu, C.H.; Li, Z.P. Rolling Circle Extension-Actuated Loop-Mediated Isothermal Amplification (Rca-Lamp) for Ultrasensitive Detection of Micrornas. *Biosens. Bioelectron.* **2019**, *128*, 17–22. [CrossRef] [PubMed]

84. Feng, X.H.; Yang, K.X.; Feng, Z.Y.; Xie, Y.F.; Han, W.J.; Chen, Q.Q.; Li, S.L.; Zhang, Y.Q.; Yu, Y.; Zou, G. Selective and Sensitive Detection of Mirna-198 Using Single Polymeric Microfiber Waveguide Platform with Heterogeneous Cha Amplification Strategy. *Talanta* **2022**, *240*, 123218. [CrossRef]

85. Mansourian, N.; Rahaie, M.; Hosseini, M. A Nanobiosensor Based on Fluorescent DNA-Hosted Silver Nanocluster and Hcr Amplification for Detection of Microrna Involved in Progression of Multiple Sclerosis. *J. Fluoresc.* **2017**, *27*, 1679–1685. [CrossRef] [PubMed]

86. Huard, D.J.E.; Demissie, A.; Kim, D.; Lewis, D.; Dickson, R.M.; Petty, J.T.; Lieberman, R.L. Atomic Structure of a Fluorescent Ag-8 Cluster Templated by a Multistranded DNA Scaffold. *J. Am. Chem. Soc.* **2019**, *141*, 11465–11470. [CrossRef] [PubMed]

87. Cerretani, C.; Kanazawa, H.; Vosch, T.; Kondo, J. Crystal Structure of a Nir-Emitting DNA-Stabilized Ag-16 Nanocluster. *Angew. Chem.-Int. Ed.* **2019**, *58*, 17153–17157. [CrossRef]

88. Geczy, R.; Christensen, N.J.; Rasmussen, K.K.; Kalomista, I.; Tiwari, M.K.; Shah, P.T.; Yang, S.W.; Bjerrum, M.J.; Thulstrup, P.W. Formation and Structure of Fluorescent Silver Nanoclusters at Interfacial Binding Sites Facilitating Oligomerization of DNA Hairpins. *Angew. Chem.-Int. Ed.* **2020**, *59*, 16091–16097. [CrossRef]

89. Nagda, R.; Park, S.; Jung, I.L.; Nam, K.; Yadavalli, H.C.; Kim, Y.M.; Yang, K.; Kang, J.; Thulstrup, P.W.; Bjerrum, M.J.; et al. Silver Nanoclusters Serve as Fluorescent Rivets Linking Hoogsteen Triplex DNA and DNA Structures. *ACS Nano* **2022**, *16*, 13211–13222. [CrossRef]

90. Jia, X.F.; Li, J.; Wang, E.K. Cu Nanoclusters with Aggregation Induced Emission Enhancement. *Small* **2013**, *9*, 3873–3879. [CrossRef]

91. Rubinstein, I.; Bard, A.J. Electrogenerated Chemiluminescence. 37. Aqueous Ecl Systems Based on Tris(2,2′-Bipyridine)Ruthenium(2+) and Oxalate or Organic Acids. *J. Am. Chem. Soc.* **2002**, *103*, 512–516. [CrossRef]

92. Zhao, G.; Wang, Y.; Li, X.; Yue, Q.; Dong, X.; Du, B.; Cao, W.; Wei, Q. Dual-Quenching Electrochemiluminescence Strategy Based on Three-Dimensional Metal-Organic Frameworks for Ultrasensitive Detection of Amyloid-Beta. *Anal. Chem.* **2019**, *91*, 1989–1996. [CrossRef] [PubMed]

93. Lu, M.-C.; Whang, C.-W. The Role of Direct Oxalate Oxidation in Electrogenerated Chemiluminescence of Poly(4-Vinylpyridine)-Bound Ru(Bpy)$_2$cl$^+$/Oxalate System on Indium Tin Oxide Electrodes. *Anal. Chim. Acta* **2004**, *522*, 25–33. [CrossRef]

94. Gao, X.; Lv, B.; Zhou, Z.; Xiao, D. Application of the Ru(Bipy)$_2$(Dpp)$^{2+}$/C$_2$o$_4$$^{2-}$ Electrochemiluminescence Reaction to the Determination of Phenol. *Mikrochim. Acta* **2007**, *161*, 163–167. [CrossRef]

95. Feng, Q.M.; Shen, Y.Z.; Li, M.X.; Zhang, Z.L.; Zhao, W.; Xu, J.J.; Chen, H.Y. Dual-Wavelength Electrochemiluminescence Ratiometry Based on Resonance Energy Transfer between Au Nanoparticles Functionalized G-C3n4 Nanosheet and Ru(Bpy)(3)(2+) for Microrna Detection. *Anal. Chem.* **2016**, *88*, 937–944. [CrossRef]

96. Tian, D.D.; Zhao, D.; Li, W.; Li, Z.H.; Zhai, M.M.; Feng, Q. Interfacial DNA/Rna Duplex-Templated Copper Nanoclusters as a Label-Free Electrochemiluminescence Strategy for the Detection of Ribonuclease H. *J. Electroanal. Chem.* **2022**, *920*, 116571. [CrossRef]

97. Guo, Y.H.; Liu, S.H.; Yang, H.L.; Wang, P.; Feng, Q.M. Proximity Binding-Triggered Multipedal DNA Walker for the Electrochemiluminescence Detection of Telomerase Activity. *Anal. Chim. Acta* **2021**, *1144*, 68–75. [CrossRef] [PubMed]

98. Wang, C.; Chen, M.; Han, Q.; Wu, J.L.; Zhao, X.; Fu, Y.Z. A Three-Dimensional DNA Nanomachine with Target Recycling Amplification Technology and Multiple Electrochemiluminescence Resonance Energy Transfer for Sensitive Microrna-141 Detection. *Biosens. Bioelectron.* **2020**, *156*, 112146. [CrossRef]

99. Feng, Q.M.; Ma, P.; Cao, Q.H.; Guo, Y.H.; Xu, J.J. An Aptamer-Binding DNA Walking Machine for Sensitive Electrochemiluminescence Detection of Tumor Exosomes. *Chem. Commun.* **2020**, *56*, 269–272. [CrossRef] [PubMed]

100. Zhang, P.; Li, Z.Y.; Wang, H.J.; Zhuo, Y.; Yuan, R.; Chai, Y.Q. DNA Nanomachine-Based Regenerated Sensing Platform: A Novel Electrochemiluminescence Resonance Energy Transfer Strategy for Ultra-High Sensitive Detection of Microrna from Cancer Cells. *Nanoscale* **2017**, *9*, 2310–2316. [CrossRef]

101. Feng, Q.M.; Guo, Y.H.; Xu, J.J.; Chen, H.Y. A Surface-Confined DNA Assembly Amplification Strategy on DNA Nanostructural Scaffold for Electrochemiluminescence Biosensing. *Biosens. Bioelectron.* **2018**, *100*, 571–576. [CrossRef]

102. Bian, X.T.; Guo, B.; Zhao, M.; Han, D.B.; Cheng, W.; Song, F.Z.; Ding, S.J. An Enzyme-Free "on-Off" Electrochemiluminescence Biosensor for Ultrasensitive Detection of Pml/Rar Alpha Based on Target-Switched DNA Nanotweezer. *ACS Appl. Mater. Interfaces* **2019**, *11*, 3715–3721. [CrossRef] [PubMed]

103. Cha, T.G.; Pan, J.; Chen, H.R.; Robinson, H.N.; Li, X.; Mao, C.D.; Choi, J.H. Design Principles of DNA Enzyme-Based Walkers: Translocation Kinetics and Photoregulation. *J. Am. Chem. Soc.* **2015**, *137*, 9429–9437. [CrossRef]

104. Feng, Q.M.; Zhao, X.L.; Guo, Y.H.; Liu, M.K.; Wang, P. Stochastic DNA Walker for Electrochemical Biosensing Sensitized with Gold Nanocages@Graphene Nanoribbons. *Biosens. Bioelectron.* **2018**, *108*, 97–102. [CrossRef]

105. Guo, Y.H.; Cao, Q.H.; Feng, Q.M. Catalytic Hairpin Assembly-Triggered DNA Walker for Electrochemical Sensing of Tumor Exosomes Sensitized with Ag@C Core-Shell Nanocomposites. *Anal. Chim. Acta* **2020**, *1135*, 55–63. [CrossRef] [PubMed]

106. Yan Jiao, H.L.; Wang, H.; Feng, Q.; Gao, Y. Proximity Hybridization Regulated Dual-Mode Ratiometric Biosensor for Estriol Detection in Pregnancy Serum. *Anal. Chim. Acta* **2023**, *1278*, 341689. [CrossRef] [PubMed]

107. Zheng, K.; Setyawati, M.I.; Leong, D.T.; Xie, J. Antimicrobial Silver Nanomaterials. *Coord. Chem. Rev.* **2018**, *357*, 1–17. [CrossRef]

108. Javani, S.; Lorca, R.; Latorre, A.; Flors, C.; Cortajarena, A.L.; Somoza, A. Antibacterial Activity of DNA-Stabilized Silver Nanoclusters Tuned by Oligonucleotide Sequence. *ACS Appl. Mater. Interfaces* **2016**, *8*, 10147–10154. [CrossRef]

109. Eun, H.; Kwon, W.Y.; Kalimuthu, K.; Kim, Y.; Lee, M.; Ahn, J.-O.; Lee, H.; Lee, S.H.; Kim, H.J.; Park, H.G.; et al. Melamine-Promoted Formation of Bright and Stable DNA-Silver Nanoclusters and Their Antimicrobial Properties. *J. Mat. Chem. B* **2019**, *7*, 2512–2517. [CrossRef]

110. Li, Q.; Wang, F.; Shi, L.; Tang, Q.; Li, B.; Wang, X.; Jin, Y. Nanotrains of DNA Copper Nanoclusters That Triggered a Cascade Fenton-Like Reaction and Glutathione Depletion to Doubly Enhance Chemodynamic Therapy. *ACS Appl. Mater. Interfaces* **2022**, *14*, 37280–37290. [CrossRef]

111. Walsh, A.G.; Chen, Z.Y.; Zhang, P. X-ray Spectroscopy of Silver Nanostructures toward Antibacterial Applications. *J. Phys. Chem. C* **2020**, *124*, 4339–4351. [CrossRef]

112. Gupta, A.K.; Marshall, N.; Yourston, L.; Rolband, L.; Beasock, D.; Danai, L.; Skelly, E.; Afonin, K.A.; Krasnoslobodtsev, A.V. Optical, Structural, and Biological Properties of Silver Nanoclusters Formed within the Loop of a C-12 Hairpin Sequence. *Nanoscale Adv.* **2023**, *5*, 3500–3511. [CrossRef] [PubMed]

113. Rolband, L.; Yourston, L.; Chandler, M.; Beasock, D.; Danai, L.; Kozlov, S.; Marshall, N.; Shevchenko, O.; Krasnoslobodtsev, A.V.; Afonin, K.A. DNA-Templated Fluorescent Silver Nanoclusters Inhibit Bacterial Growth While Being Non-Toxic to Mammalian Cells. *Molecules* **2021**, *26*, 4045. [CrossRef] [PubMed]

114. Gao, L.; Zhuang, J.; Nie, L.; Zhang, J.; Zhang, Y.; Gu, N.; Wang, T.; Feng, J.; Yang, D.; Perrett, S.; et al. Intrinsic Peroxidase-Like Activity of Ferromagnetic Nanoparticles. *Nat. Nanotechnol.* **2007**, *2*, 577–583. [CrossRef] [PubMed]

115. He, W.; Wamer, W.; Xia, Q.; Yin, J.-j.; Fu, P.P. Enzyme-Like Activity of Nanomaterials. *J. Environ. Sci. Health Part C-Environ. Carcinog. Ecotoxicol. Rev.* **2014**, *32*, 186–211. [CrossRef]

116. Zheng, C.; Zheng, A.-X.; Liu, B.; Zhang, X.-L.; He, Y.; Li, J.; Yang, H.-H.; Chen, G. One-Pot Synthesized DNA-Templated Ag/Pt Bimetallic Nanoclusters as Peroxidase Mimics for Colorimetric Detection of Thrombin. *Chem. Commun.* **2014**, *50*, 13103–13106. [CrossRef]

117. Wu, L.-L.; Wang, L.-Y.; Xie, Z.-J.; Pan, N.; Peng, C.-F. Colorimetric Assay of L-Cysteine Based on Peroxidase-Mimicking DNA-Ag/Pt Nanoclusters. *Sens. Actuator B-Chem.* **2016**, *235*, 110–116. [CrossRef]

118. Mu, X.M.; Li, J.S.; Xiao, S.X.; Xu, J.Y.; Huang, Y.; Zhao, S.L.; Tian, J.N. Peroxidase-Mimicking DNA-Ag/Pt Nanoclusters Mediated Visual Biosensor for Cea Detection Based on Rolling Circle Amplification and Crispr/Cas 12a. *Sens. Actuator B-Chem.* **2023**, *375*, 1322870. [CrossRef]

119. Borghei, Y.-S.; Hosseini, M.; Ganjali, M.R. Visual Detection of Mirna Using Peroxidase-Like Catalytic Activity of DNA-Cuncs and Methylene Blue as Indicator. *Clin. Chim. Acta* **2018**, *483*, 119–125. [CrossRef]

120. Du, Z.; Wei, C. Using G-Rich Sequence to Enhance the Peroxidase-Mimicking Activity of DNA-Cu/Ag Nanoclusters for Rapid Colorimetric Detection of Hydrogen Peroxide and Glucose. *ChemistrySelect* **2020**, *5*, 5166–5171. [CrossRef]

121. Li, S.; Zeng, Z.; Zhao, C.; Wang, H.; Ye, X.; Qing, T. Nucleoside-Regulated Catalytic Activity of Copper Nanoclusters and Their Application for Mercury Ion Detection. *New J. Chem.* **2022**, *46*, 4687–4692. [CrossRef]

122. Ji, Z.; Ji, Y.; Ding, R.; Lin, L.; Li, B.; Zhang, X. DNA-Templated Silver Nanoclusters as an Efficient Catalyst for Reduction of Nitrobenzene Derivatives: A Systematic Study. *Nanotechnology* **2021**, *32*, 195705. [CrossRef] [PubMed]

123. Guo, Y.; Ren, J.; Wang, E. Implementation of Logic Operations and Bioanalysis Based on DNA Allostery-Regulated Nanometallic Catalysis. *Nano Today* **2022**, *44*, 101476. [CrossRef]

124. Chakraborty, S.; Babanova, S.; Rocha, R.C.; Desireddy, A.; Artyushkova, K.; Boncella, A.E.; Atanassov, P.; Martinez, J.S. A Hybrid DNA-Templated Gold Nanocluster for Enhanced Enzymatic Reduction of Oxygen. *J. Am. Chem. Soc.* **2015**, *137*, 11678–11687. [CrossRef]

125. Luo, W.; Wu, S.; Jiang, Y.; Xu, P.; Zou, J.; Qian, J.; Zhou, X.; Ge, Y.; Nie, H.; Yang, Z. Efficient Electrocatalytic Nitrate Reduction to Ammonia Based on DNA-Templated Copper Nanoclusters. *ACS Appl. Mater. Interfaces* **2023**, *15*, 18928–18939. [CrossRef] [PubMed]